의학박사 학위논문

Studies on Characteristics of CD8 T cell Response for Minor Histocompatibility Antigen, H60 and Role of Myeloid cells in the Development of T cell Response

부조직적합항원 H60 특이적 CD8 T 세포 반응의 특성과 CD8 T 세포 반응 발달에서 골수계 세포의 역할 연구

2016 년 02 월

서울대학교 대학원

의과학과 의과학 전공

류 수 정

A thesis of the Degree of Doctor of Philosophy

부조직적합항원 H60 특이적 CD8 T 세포 반응의 특성과 CD8 T 세포 반응 발달에서 골수계 세포의 역할 연구

Studies on Characteristics of CD8 T cell Response for Minor Histocompatibility Antigen, H60 and Role of Myeloid cells in the Development of T cell Response

February 2016

The Department of Biomedical Sciences,

Seoul National University

College of Medicine

Sujeong Ryu

ABSTRACT

The balance between immunity and tolerance is required to maintain immune homeostasis. Understanding how tolerance can be induced extrathymically has important implication for attempts to establish a nonresponsive state to allogeneic antigens borne on tissue grafts and for reestablishing self-tolerance in patients suffering from autoimmune disease. In this study, I investigated whether the induction of help-deficient CD8 T cell response for H60 could generate memory impairment of the H60-specific CD8 T cells and whether the memory impairment of CD8 T cell specific for H60, the most dominant minor H antigen, would influence the immune hierarchy of CD8 T cells specific for other minor H antigens. Helper-deficient CD8 T cells show reduced burst expansion and the tolerance of H60-specific CD8 T cells has rendered CD8 T cells specific for other minor H antigens to be tolerized as well, reducing the total intensity of allo-response induced after transplantation.

To understand the thymic selection process for H60-specific CD8 T cells and control of the specific response, I investigated

the effect of a single amino acid substitution in the H60 epitope on the composition of the TCR repertoire. These results demonstrated that some overlap in TCR usage between CD8 T cells responding to H60H vs. H60N stimulation, suggesting that the H60H epitope will be useful for understanding the selection process and control of CD8 T cells specific for H60.

In the third part, I showed that differentiation of transplanted Lin^- cells into myeloid-derived suppressor cells inflamed skin to be the basis of the alleviation of skin inflammation after Lin^- cell transplantation. Taken together, these results provide insight for modeling therapeutic applications to control CD8 T cell response.

Keywords: minor histocompatibility antigen, CD4 help, immune tolerance, memory CD8 T cells, TCR repertoires, Myeloid-derived suppressor cells.

Student number: 2009-21884

CONTENTS

LIST OF TABLES AND FIGURES

Chapter 1

Chapter 2

Chapter 3

LIST OF ABBREVIATION

m H Ag: minor histocompatibility antigen

MHC: major histocompatibility complex

TCR: T cell antigen receptor

MDSC: myeloid-derived suppressor cells

TEM: Effector memory T

TCM: Central memory T

GVHD: graft versus host disease

GVL: graft versus leukemia

CTL: cytotoxic T lymphocyte

APLs: altered peptide ligands

Lin: Lineage

HSCs: hematopoietic stem cells

LN: lymph node

i.p.: intraperitoneal injection

s.c: subcutaneous injection

i.v: intravenous

PBLs: peripheral blood lymphocytes

MLC: mixed lymphocytes culture

Ab: antibody

CHAPTER 1

Effects of CD8 T cell tolerance to dominant minor histocompatibility Ag on the response to subdominant antigens in MHC-matched transplantation

INTRODUCTION

CD8 T cells play a major role in cell-mediated immune responses. They protect the body responding to infection of pathogens and are also involved in the rejection of allogeneic transplants. These functions are performed after interaction with antigen-presenting cells expressing major histocompatibility complex (MHC) class I molecules that present peptides derived from pathogens or allogeneic antigens. CD8 T cell responses after recognition of foreign antigens from pathogens or allo-grafts develop within three phases: clonal expansion and differentiation into effector cells of the activated T cells, contraction of the expanded effector cells, and memory cell generation [1].

In a conventional development course of CD8 T cell response, help conferred by activated CD4 T cells has been known to play critical roles, ensuring induction of CD8 T cell response for non-inflammatory cell-based antigens (help-dependent response) [2]. Additionally, CD4 T cell help exerts influence on the fate decisions of memory precursor effector cells (MPEC: IL-7Rα^{hi}KLRG-1^{low}) or short term lived effector cells (SLEC: IL-7Rα^{hi}KLRG-1^{low}) [3], generation of memory cells,

and long term homeostatic survival of the generated memory cells [2]. Thus, memory expansion of CD8 T cells was impaired against re-infection even with inflammatory pathogens which are known to be help-independent for the induction of primary response [2].

Despite these various impacts of CD4 help on CD8 T cell response reported, the key mechanisms underlying and unifying all these phenomena have not yet been clearly comprehended. Previous studies have shown that CD4 help is delivered via CD40/CD40L-mediated interactions between CD4 T cells antigen presenting cells (APCs) [4, 5] and via CD70/CD27-mediated interaction between CD8 T cells and APCs [6].

In a few studies using help-dependent cellular antigen models, it has been reported that expansion of antigen-specific CD8 T cells was impaired when CD4 T cell help was not provided during the induction of primary response [7, 8]. CD4-depleted mice did not show primary expansion of antigen-specific CD8 T cells, tolerated male grafts [8] and heart transplant expressing OVA antigen [7], or failed in tumor surveillance, with non-responsiveness to further antigen-stimulation [2]. Impairment of memory expansion of CD8 T

cells was also observed when the CD8 T cells activated in the absence of CD4 help were re-exposed to the same antigen, regardless of the help-dependent or -independent nature of the antigen [2, 9]. These findings suggested that CD4 help would encode a program in activated CD8 T cells to generate memory cells. When re-stimulated, the help-deficient CD8 T cells were found to die of TRAIL-mediated or up-regulate PD-1, suggesting the role of TRAIL or PD-1 in impairment of memory CD8 T cell expansion [10]. However, such memory impairment of CD8 T cell primed in the absence of CD4 help was still observed in TRAIL-deficient mice [11], indicating the irrelevance of TRAIL-mediated cell death in the defect in memory impairment. Molecular and cellular mechanisms for activated CD4 T cells to help CD8 T cell response have remained obscure. And questions regarding exactly how CD4 help-deficiency would have CD8 T cell response deviate from the conventional differentiation path and gain defective attributes still remain unanswered.

Development of help-deficient CD8 T cell response has never been thoroughly dissected, especially with the help-dependent cellular antigen model, mainly because of low

numbers of expanded CD8 T cells during the response induced under help-deficient condition. To address the helper-dependent nature of the CD8 T-cell response under physiological conditions using natural cellular model antigens, I exploited a system in which the CD8 T-cell responses were induced against minor histocompatibility (H) antigens via MHC-matched transplantation between C57BL/6 (B6) and BALB.B strains of mice. Minor H antigens are naturally processed peptides with a polymorphism at the epitope fragments presented by MHC class I and II and recognized as foreign epitopes after allogeneic transplantation. BALB.B mice, MHC-matched but mismatched for different background genes with B6 mice, express very high numbers of allo-antigens arising from genes encoding polymorphic proteins [12]. Even though exposure of high numbers of foreign antigens to an immune system could generate complicated immune responses for the allo-antigens, immune responses are known to be focused on a few dominant antigens, generating immune hierarchy among different allo-antigens [13]. H60 has been known to be exceptionally immune dominant, for which response dominate over the responses for several different

identified dominants antigens and takes account of 70-80 % of allo-responses of B6 mice against BALB.B cells [14]. Moreover, the single H-2K^{b}-presented H60 peptide (LTFNYRNL) could elicit a CD8 T-cell response competing even with the response against allo-MHC [14] [15]. However, this immunodominance is CD4 T-helper cell dependent. Thus, the specific CD8 T-cell response becomes subservient in the absence of concomitant activation of CD4 T cells. This critical feature provided the rationale for the use of H60 as a model antigen to investigate the effects of CD4 T cells on the CD8 T-cell response.

The B6.CH60 mouse strain has congenic H60 region in a B6 background on chromosome 10. This region provides the H60-CD8 epitope to T cells in the B6 strain, which does not express H60. In addition, Hy-Dby locus at the Y-chromosome provides H-2A^{b}-restricted CD4 epitope (NAGFNSNRANSSRSS). Thus, usage of female or male H60 congenic strain of mice as an allogeneic donor to induce H60-specific CD8 T cell response in female B6 mice enabled production of help-deficient or -sufficient conditions for the CD8 T cells activated against H60 epitope (LTFNYRNL) presented by H-2K^{b}, respectively. Using

this system, I have reported the requirement of CD40-CD40L-mediated CD4 help for the induction of primary and memory expansions of H60-specific CD8 T cells [16], and recruitment of diverse T-cell receptors (TCRs) to the specific CD8 T-cell response [17]. In addition, I have shown that memory expansion of H60-specific CD8 T cells heavily depended on CD4 help provided during the re-challenge.

In this study, I investigated whether the induction of help-deficient CD8 T cell response for H60 could generate memory impairment of the H60-specific CD8 T cells and whether the memory impairment of CD8 T cell specific for H60, the most dominant minor H antigen, would influence the immune hierarchy of CD8 T cells specific for other minor H antigens. And the results from this study will demonstrate that H60-specific CD8 T cells become tolerized when the primary response is induced under help-deficient condition and the tolerance of H60-specific CD8 T cells has rendered CD8 T cells specific for other minor H antigens to be tolerized as well, reducing the total intensity of allo-response induced after BALB.B cell immunization.

MATERIALS AND METHODS

1. Mouse

C57BL/6 (B6), C.B10-H2^{b}/LiMcdJ (BALB.B), B6.SJL-Ptprc ^{b} Pep3^{a}/BoyJ (CD45.1^{+}) and B6.C-H60c/DCR (B6.CH60) mice were obtained from the Jackson Laboratory (BarHarbor, ME, USA). TCR transgenic mouse lines with TCR specific to the H60-CD8 epitope/H-2K^{b} were generated after microinjection of a fertilized B6 egg with eukaryotic DNA fragments from pTα and pTβ cassette plasmids [18] containing TCRVα-Jα and TCRVβ-Dβ-Jβ rearranged genomic sequences originating from H60-specific CTL clone 15 [19], respectively. The transgenic mice were generated by injection of linearized DNA fragments devoid of prokaryotic sequences into fertilized eggs of B6 mice. Transgenic founders were identified by PCR analysis of genomic DNA and flow cytometric analysis of PBLs after staining with anti-Vβ8.3 Ab. Among the three founder lines showing positive selection on a B6 background and negative selection on a B6.CH60, I selected one line ([19]; designated J15) in which the TCR levels on circulating blood CD8 T cells were comparable to those of wild-type B6 T cells.

All mice were maintained under specific pathogen-free conditions at the Bio medical Center for Animal Resource Development of Seoul National University College of Medicine, Korea and used for experiments at ages of 8-12 weeks with the approval of the Institutional Animal Care and Use Committee (IACUC) of Seoul National University.

2. Adoptive transfer and immunization

CD8 T cells from CD45.1 mice were purified from spleens and LNs by negative MACS (MACS; Milgenyl Biotec, Auburn, CA, USA) and were adoptively transferred (3×10^6) on day before priming. 2×10^7 B6.CH60 cells were injected i.p. to induce H60-specific CD8 T cell response.

3. Antibodies and Flow cytometry

Single cells were stained with Abs, H60-tetramers (LTFNYRNL/H-2Kb) in staining buffer (1xPBS containing 0.1% bovine serum albumin and 0.1% sodium azide). Intracellular staining was performed as previously described. Cells were run on FACSCalibur (BD Pharmingen, San Diego, CA, USA) or LSRII-Green (BD pharmingen) and data were analyzed with

FlowJo software (Tree Star, Ashland, OR, USA). Abs used for flow cytometric analysis are as follows. Fluorescent-dye-conjugated Abs against CD8, CD45.1, Annexin, CD25, Fas, CD40, CD40L, IgM and IFN-γ were purchased from eBiosciences (San Diego, CA, USA). Other Abs were purchased from BD pharmingen (anti-CD11a and anti-PD-1 Abs).

4. Statistical analysis

Statistical analysis was performed using GraphPad Prism (version 5, GraphPad Software, La Jolla, CA, USA). All error bars represent the standard error of the mean (SEM). P values were determined by Student's t-tests. (Unpaired two-tailed: $*P < 0.05$, $**P < 0.01$, $***P < 0.001$)

RESULTS

Induction of tolerance of H60-specific CD8 T cell response by lack of CD4 help during primary response

In order to investigate the influence of CD4 help on H60-specific memory CD8 T cell expansion, I examined whether H60-specific CD8 T cells would become non-responsive to secondary antigen stimulation, when the specific CD8 T cells were primed under help-deficient condition [2, 7, 8]. Female B6 mice were primed with female H60 congenic splenocytes for induction of help-deficient primary response and, then, re-challenged with male H60 congenic splenocytes 40 days later to induce a secondary response, providing H60-CD8 epitope and Hy-Dby CD4 epitope.

PBLs from the primed-and-boosted mice were periodically checked for expansion of the H60-specific CD8 T cells by H60-tetrmaer-staining and subsequent flow cytometric analysis (Fig. 1A, B). During the longitudinal analysis, CD8 T cells binding to H60-tetramer were not detected at significant levels in the blood from help-deficient group over the period encompassing the primary and secondary responses. Frequencies of the H60-tetamer-binding cells ranged 0.1-1 %

of CD8 T cells in the blood from the help-deficient mice (just 1.7-fold average increase compared to the primary peak frequencies) on day 7 post-boost when they peaked as 40 - 50% (5-7-fold increase) in the helped-and-boosted group (Fig. 1A). Additionally, when female B6 hosts were primed with 3-fold-enhanced dose of female H60 congenic splenocytes (3 x help-deficient; Fig. 1) to examine if increase in antigen load could compensate the lack of CD4 help, memory expansion was observed to be negligible again and rather compromised by the elevated antigen load (Fig. 1). The numbers of H60-specific CD8 T cells in the spleens of the help-deficient (both 1 x and 3 x)-and-boosted mice were extremely low (Fig. 1B). Priming of GK-1.5-mediated CD4-depleted hosts with male H60 congenic splenocytes also led to the non-responsiveness to the boosting with male H60 congenic splenocytes (Fig. 1C). With these results, I could conclude that induction of H60-specific CD8 T cell response under help-deficient condition established non-responsiveness or tolerance to re-encounter of H60.

NKG2D has been reported to assist memory response of helpless CD8 T cells [20], which raised a suspicion that protein function of H60 as a ligand of activating receptor NKG2D might

play some role in the tolerance process. To rule out any influence from H60 protein function itself, I primed female B6 mice with cells pulsed with peptides corresponding to H60-CD8-epitope only (help-deficient) or together with HY-Dby-CD4-epitope (helped), and boosted them with male H60 congenic splenocytes 40 days later. In the longitudinal flow cytometry analysis, frequencies of H60-tetramer-binding CD8 T cells were low in the blood from the mice primed in the peptide version during the primary response, regardless of the help-providing and -deficient conditions. However, the frequencies were encouraged up to 10% of CD8 T cells in the blood by the additional boost with male H60 congenic splenocytes only in the helped case, not in the help-deficient case (Fig. 1D). Therefore, this confirmed that recognition of H60-peptide/MHC complex by the specific CD8 T cells, not the H60 protein function itself, is the basis for the tolerance induction during in the help-deficient CD8 T cell response.

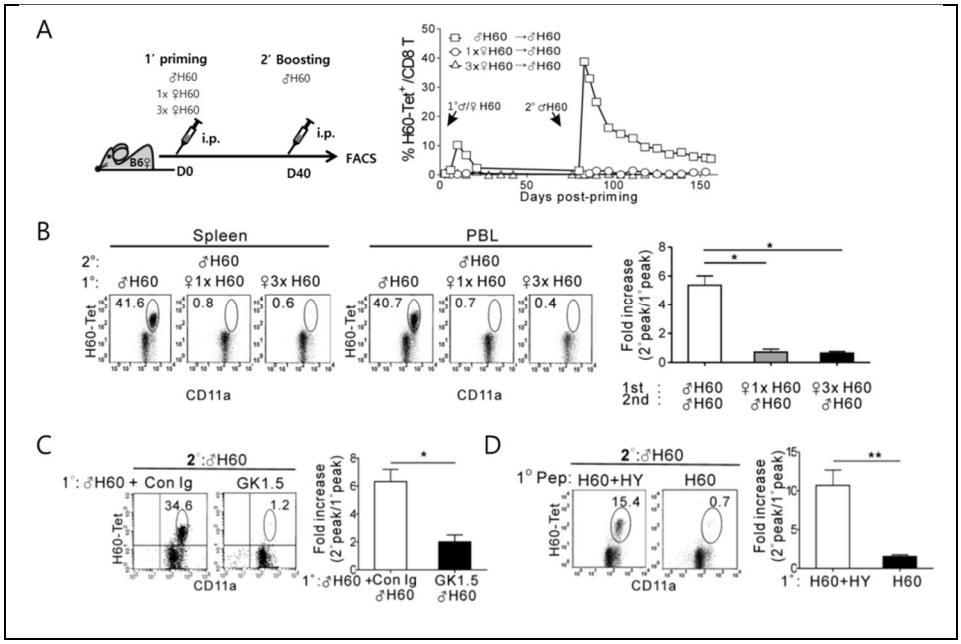

Figure 1. Impairment of memory expansion of H60-specific $CD8^+$ T cells activated in the absence of $CD4^+$ T-cell help.

(A) Diagrams of experimental systems using B6.CH60 mice. The B6 mouse strain has null expression in the H60 locus, whereas the B6. H60 strain expresses H60C allele at the locus, which produces the H-$2K^b$-restricted CD8 epitope to activate T cells of B6 mice. The Hy-Dby gene on the Y chromosome encodes the CD4 epitope presented by H-$2A^b$. Priming of female B6 mice with female or male cells from B6.CH60 mice induces the helper-deficient of helped response for H60, respectively. (B) Female B6 mice were primed with splenocytes of female B6.CH60 mice at a 1x dose (2×10^7) or

a 3x dose (6 x 10^7), or with male (2 x 10^7) B6. CH60 spleen cells, and then boosted with male B6. CH60 spleen cells (2x10^7). Pooled PBLs from three immunized mice were analysed periodically using flow cytometry after staining with H60 tetramers, and anti-CD11a and anti-CD8 monoclonal antibodies (mAbs). The frequencies of H60-tetramer-binding cells in blood $CD8^+$ T cells were then plotted. (C) Flow cytometric data of splenocytes and PBLs obtained on day 7-post boosting are shown after $CD8^+$ gating, with percentages of the H60-tetramer binding cells in $CD8^+$ T cells denoted. The fold increases in the frequency of the secondary peak (day 7 post boosting) relative to that of the primary peak (day 10 post priming) is shown. (D) Female B6 mice treated with GK1.5 or control Ig were primed with male B6.CH60 cells. (E) Female B6 mice were primed with female syngeneic cells loaded with the H60 peptide alone or combined with the HY-Dby peptide. Then, these primed mice (D) were boosted with male B6. CH60 cells 40 days later. Representative date from flow cytometric analysis of PBLs from the boosted mice on day 7 post boosting are shown, with the plots of the fold increase in the frequency. All data (B) are representative of more than three independent

experiments (n=3 per group per experiment). Data are presented as means± SEM $*P < 0.05$, $**P < 0.01$ determined by Student's t-test.

Functional activity of H60-specific CD8 T cells is impaired by experience of CD4 help deficiency

Next, functional activity of the H60-specific CD8 T cells in the tolerized-and-boosted mice was evaluated via *ex vivo* IFN-γ-secretion and *in vivo* cytotoxic analyses. Results showed that the percentages of splenic CD8 T cells producing IFN-γ in response to H60-stimulation *in vitro* were significantly low (Fig. 2A) and specific killing of target cells presenting H60-peptide did not occur *in vivo* in the tolerized-and-boosted mice (Fig. 2B). These data were in a sharp contrast with appropriate functional activity of splenic CD8 T cells in helped-and-boosted mice. These results demonstrated that not only memory expansion but also functional activity of H60-specific CD8 T cells was impaired in the tolerized-and-boosted mice.

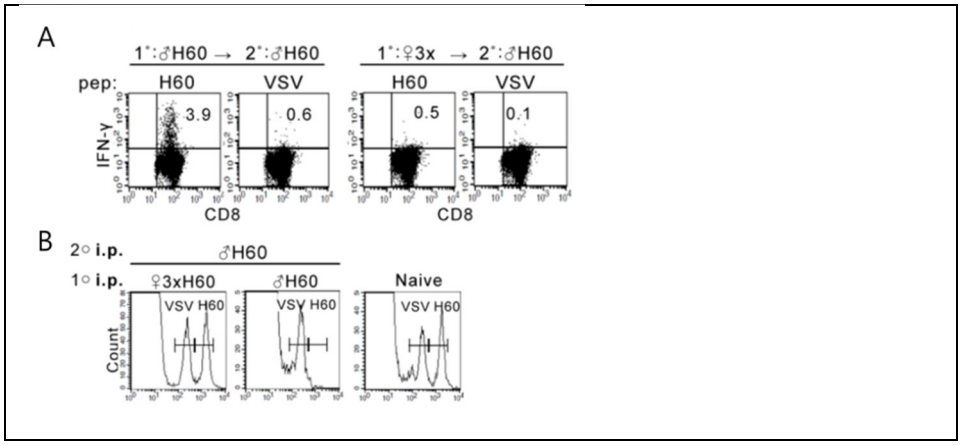

Figure 2. Impairment of function of H60-specific CD8 T cells under help deficient conditions.

(A) Specific IFN-γ production was assessed in splenocytes harvested from tolerized-and-boosted or helped-and-boosted hosts on day 7 post boosting. (B) In vivo cytotoxicity assay. Mixtures (1:1) of the carboxyfluorescein N-succinimidyl ester (CFSE)-labeled and peptide-loaded target cells (2.5 mM CFSE-labeled and H60-loaded versus 0.42 mM CFSE-labelled and VSV-loaded) were i.v. injected into each group of mice and analyzed 72 h later by flow cytometry of the PBLs for detection of the CFSE-labeled cells.

Memory impairment of help-deficient H60-specific CD8 T cells in various priming and boosting methods

Next, I investigated whether impairment of memory response of help-deficient H60-specific CD8 T cells would be recapitulated with different priming and boosting methods, such as subcutaneous injection and skin grafting. Priming through s.c. injection of female H60 congenic splenocytes or skin graft also led to the non-responsiveness to the boosting with male H60 congenic splenocytes (Fig 3A, C). Specific killing of target cells presenting H60-peptide did not occur appropriately in the tolerized-and-boosted mice in s.c injection or skin graft model, either (Fig. 3B. D). With these various results from the H60-antigen model system, I could conclude that induction of H60-specific CD8 T cell response under help-deficient condition established non-responsiveness or tolerance to re-encounter, regardless of priming and boosting methods.

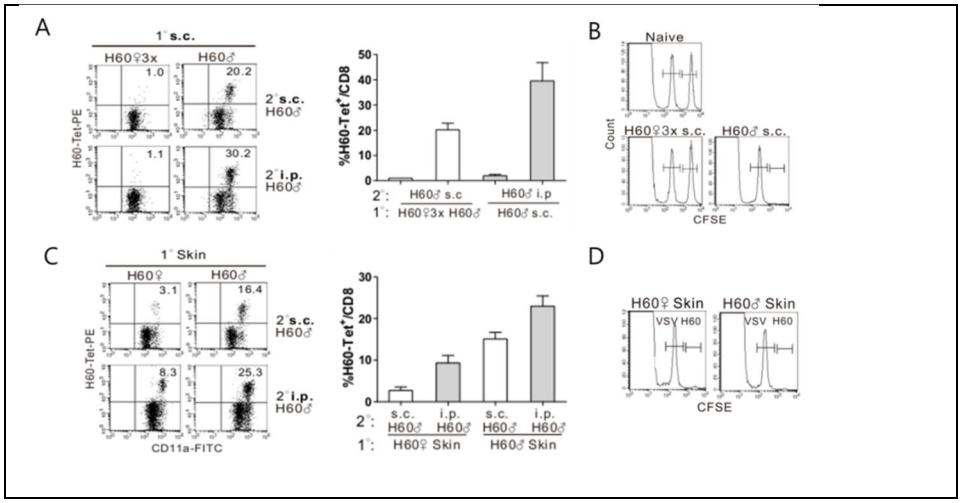

Figure 3. In the various priming and boosting method, H60-specific CD8 T cell response is impaired under helper-deficient conditions

(A-D) Female B6 mice that had been primed through s.c. injection of female or male B6.CH60 spleen cells or skin graft were boosted with male B6.CH60 spleen cells. Flow cytometric data of splenocytes and PBLs obtained on day 7-post boosting are shown after $CD8^+$ gating, with percentages of the H60-tetramer binding cells in $CD8^+$ T cells denoted. (B, D) *In vivo* cytotoxicity assay. Mixtures (1:1) of the CFSE-labeled and peptide-loaded target cells (2.5 mM CFSE-labeled and H60-loaded versus 0.42 mM CFSE-labeled and VSV-loaded) were i.v. injected into each group of mice and analyzed 72 h later by flow cytometry of the PBLs for detection of the CFSE-labeled cells.

Expansion of naïve CD8 T cells is impaired in the mice in which H60-specific CD8 T cell response has been induced under CD4 help-deficient condition

I questioned whether naive CD8 T cells which recently emigrated from thymus and, therefore, have not experienced H60 foreign antigen could respond to H60-stimulation in the mice in which tolerance to H60 had been established by female H60 spleen cell priming. To answer this question, I isolated CD8 T cells from naïve CD45.1 mice, and adoptively transferred them into the naïve mice or mice which have previously been immunized with female H60 congenic splenocytes. Then, adoptive hosts were immunized with male H60 congenic splenocytes 1 day after the adoptive transfer (Fig. 4A). Interestingly, the frequencies of CD8 T cells binding to H60-tetramer were significantly low in the mice after male H60 cell injection in which H60-specific CD8 T cells had been tolerized by immunization of female H60 congenic splenocytes, compared to those in the naïve mice (Fig. 4B). These results demonstrated that CD8 T cell response to H60 was suppressed in the mice that had been immunized with female H60 cells, regardless of their experience for CD4 help deficiency. I

speculated that the tolerance phenomenon observed in the mice primed against H60 under help-deficient condition might establish an extrinsic environment suppressing CD8 T cell response.

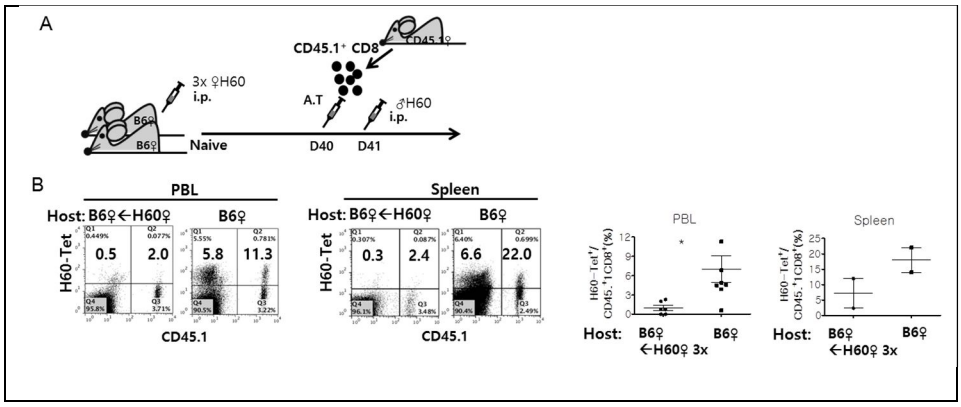

Figure 4 Expansion of naïve CD8 T cells is impaired in the mice in which H60-specific CD8 T cell response has been induced under CD4 help-deficient condition

(A)CD45.2^{+} female B6 mice were primed with female or male B6.CH60 splenocytes 40 days previously. Then, CD8^{+} T cells (3 x 10^{6}) purified from unprimed naïve CD45.1^{+} mice were adoptively transferred to female CD45.2^{+} B6 mice. Then, the adoptive hosts were challenged with male B6.CH60 splenocytes. PBLs were longitudinally analyzed after gating on CD8^{+} cells. Representative flow cytometric data obtained on day 10 post challenge are presented.

Verification of lack of expansion of naïve J15− CD8 T cells in the host primed with female H60 splenocytes

To verify the tolerance phenomenon observed in the mice primed against H60 under help−deficient condition using *in vivo* imaging, I isolated CD8 T cells from the spleen of naïve Luc−J15 mice, adoptively transferred them into B6.albino host, which had been primed against H60 under help−deficient condition, and challenged the adoptive hosts with male H60 congenic splenocytes. Then, challenged adoptive hosts were analyzed to detect Luc−J15 CD8 T cells in the body and blood (Fig. 5). Impaired expansion of luciferase−expressing J15 (J15−LucTg) CD8 T cells in the host primed with female H60 cells was further visualized by longitudinal BLI analysis of helper−deficient primed hosts into which J15−LucTg CD8 T cells were adoptively transferred (Fig. 5). The frequencies of J15 CD8 T cells also were 6.2% of J15 CD8 T cells in blood of control adoptive hosts with CD8 T cells from naïve mice, on day10 post−challenge, but were significantly low (0.44%) in the mice that had been primed with female H60 cells (Fig. 5B). These results suggest that the tolerant environment was

established in the mice had primed with female H60 cells (help−deficient).

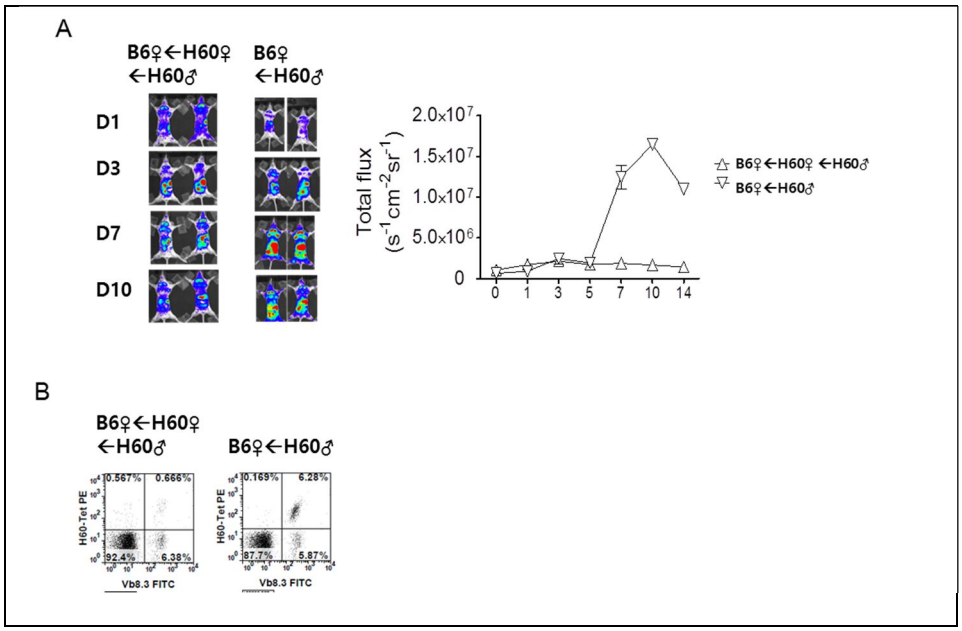

Figure 5 Verification of lack of expansion of naïve J15-CD8 T cells in the host primed with female H60 splenocytes

Dynamics of J15-LucTg CD8 T cells in B6-albino-adoptive hosts were monitored periodically after secondary challenge. (A) Photon flux values were plotted after designating the whole body as the ROI. (B) PBLs taken from the immunized mice on day 7 post-immunization were stained with tetramer PE in combination with APC- conjugated anti-CD8 mAb and FITC-conjugated anti-CD11a mAb for flow cytometry.

Tolerance of H60-specific CD8 T cells suppress expansion of CD8 T cells specific for subdominant histocompatibility antigens

Since CD8 T cell specific for H60 is dominant in the CD8 T cell responses during graft-vs-host disease in BALB.B mice after transplant of B6 BM and splenocytes [21] [15], I questioned whether tolerance induction in CD8 T cell response for H60 could ameliorate GVHD in the recipient BALB.B mice. To address this question, lethally irradiated BALB.B were transplanted with BM and splenocytes originated from B6 mice which had been immunized with female B6.CH60 mice to induce tolerance of H60-specific CD8 T cells, For controls, BM and splenocytes from naïve B6 mice or B6 mice which had been immunized with male B6.CH60 mice to generate memory CD8 T cells specific for H60 were transplanted to BALB.B (Fig 6A). In addition, those from B6.CH60 mice were transplanted to BALB.B, as MHC-and H60-matched control.

When the BALB.B recipients were tracked for disease score and survival, it was found that GVHD was significantly ameliorated in the BALB.B mice that received BM and splenocytes from B6 mice tolerized for H60. Survival was significantly enhanced with reduced disease score (Fig. 6B,C).

However, the recipients of BM and splenocytes from B6.CH60 (MHC and H60-matched) donors showed enhanced survival rate to those observed with H60-primed or naïve BM and splenocytes. When leukocytes present in blood, spleens and livers of each recipient were stained with H60-and H4-tetramers, H60-tetramer-binding CD8 T cells were detected in those from the recipients of H60-immunized group, or naïve group. Interestingly, H4-tetramer-binding CD8 T cells were not detected in the recipient of H60-tolerized group (Fig. 6D). These findings demonstrated that expansion of H60-specific CD8 T cells were dominant when donors were naïve, H60-immunized, or H60- and MHC-matched, and CD8 T cells specific for H4 expanded significantly. However, when H4 donor was tolerized against H60, the CD8 T cell response for H4 was tolerized as well.

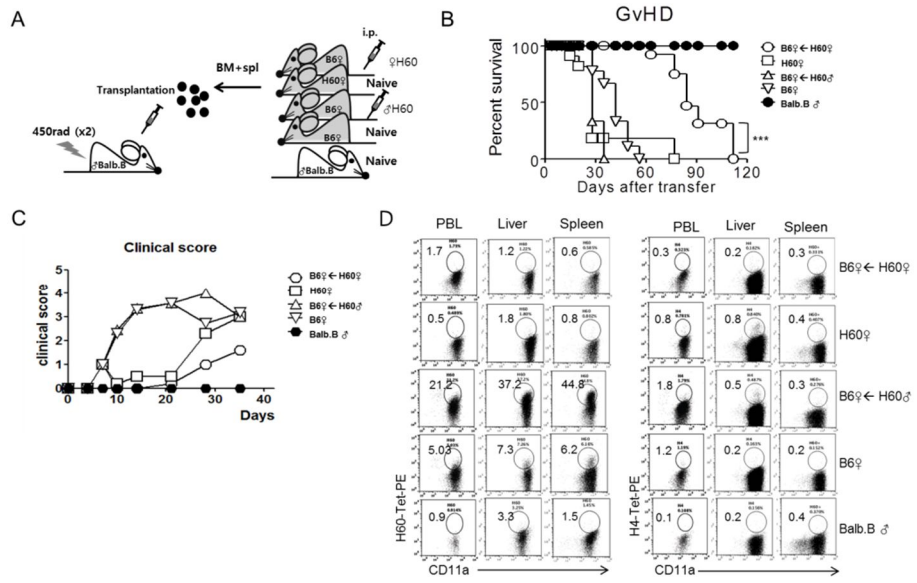

Figure 6 Tolerance of H60-specific CD8 T cells suppress expansion of CD8 T cells specific for subdominant histocompatibility antigens

(A)Experimental scheme of GVHD. BALB.B GVHD hosts were transplanted with bone marrow cells (5 x 10^6) and splenocytes (2 x 10^7) from female B6, female B6.CH60 or female B6 that had been primed with male or female B6.CH60. (B)Survival graph (C) Clinical score. (D) PBLs were stained with H60-, H4-, or H7-tetramer-PE, anti-CD8-APC and anti-CD11a-FITC Abs.

Tolerance spreading to CD8 T cell responses specific for subdominant histocompatibility antigens

Then, I questioned whether tolerance of H4-specific CD8 T cell expansion observed in the GVHD mice that received BM and splenocytes from H60-tolerized B6 mice would be related to H60-dominance in immune hierarchy. It has been reported that H60-specific CD8 T cell response is subdominant to CD8 T cell response for H4 during skin rejection in B6 mice grafted with BALB.B skin [22]. Therefore, I grafted BALB skin onto H60-tolerized mice to see whether expansion of H4-specific CD8 T cells would be impaired. The same BALB skin was transplanted onto naïve H60-immunized mice, or B6.CH60 (MHC-matched and H60-matched) recipient. In all the experimental groups, H4-tetramer binding CD8 T cells were detected, while H60-tetramer-binding CD8 T cells were detected only in the H60 immunized or naïve recipient (Fig.7). These results demonstrated that even though H60-specific CD8 T cell tolerance was maintained after BALB.B skin, H4 specific CD8 T cells could expand when H60-specific CD8 T cell response was subdominant. Thus, H60 specific CD8 T cell tolerance mediated suppression of H4-specific CD8 T cell

expansion is a phenomenon dependent on H60-immunodominancy.

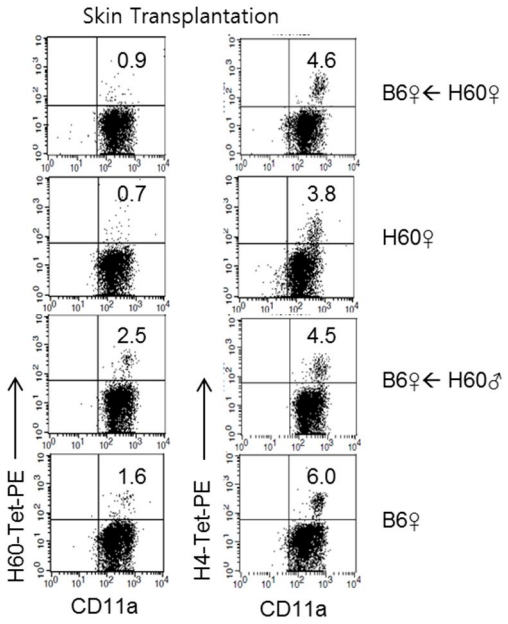

Figure 7. Spreading of tolerance to subdominant histocompatibility antigens specific CD8 T cell response

Mice were primed with splenocytes from male or female H60 mice 30 days prior to skin transplantation. Tail skins of male BALB.B skin were transplanted. PBLs were stained with H60-or H4-tetramer-PE, anti-CD8-APC and anti-CD11a-FITC Abs.

Influence of H60-specific CD8 T cell tolerance on the immune hierarchy

In an experimental setting where hematopoietic cells were major immunogenic sources, such as BALB splenocytes immunization and GVHD, CD8 T cell response for H60 have been considered to be dominant over that for H4. To investigate the impact of H60-specific CD8 T cell tolerance on the immune hierarchy in a H60-domiannt experimental setting, B6 female mice that have been immunized with female H60 congenic splenocytes were i.p injected with BALB.B splenocytes and expansion of H60-specific or H4-specific CD8 T cells were analyzed by flow cytometry (Fig. 8A). Naïve B6 mice i.p injected with BALB.B splenocytes were included as control. The frequencies of CD8 T cells binding to H4-tetramers were significantly low in the mice after BALB cell injection in which H60-specific CD8 T cells had been tolerized by immunization of female H60 congenic splenocytes, compared to those in the BALB.B immunized naïve mice (Fig. 8B). IFN-γ production of specific CD8 T cells was also rarely detected in the H60-tolerized mice (Fig. 8C). Then I performed analysis of tetramer binding and IFN-γ secretion using CD8 effector cells from

mixed lymphocyte culture (MLC). The purpose was first to amplify in vitro the CD8 T cells reactive to minor H antigen in vivo, especially those perhaps present in the help-deficient mice, and second to test whether tetramer-binding cells from the in vitro amplification would represent functionally active CD8 T cells. MLCs were performed using splenocytes from the immunized mice and irradiated male BALB.B splenocytes. The inappropriate expansion and IFN- γ production of the CD8 T cells specific for subdominant minor H antigens were reproduced when the MLC cells were analyzed (Fig. 8D).

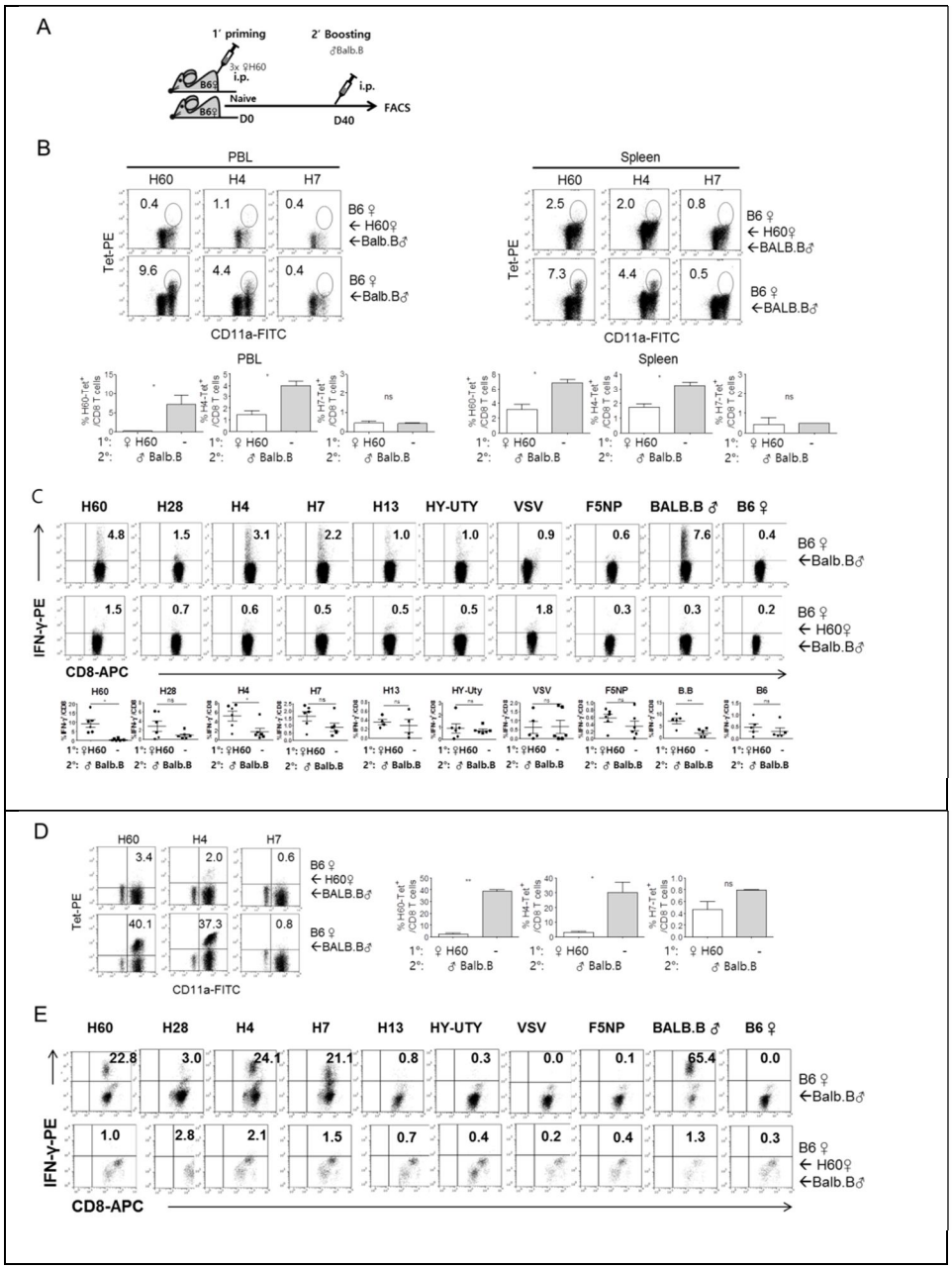
A
1° priming
2° Boosting
♂Balb.B
3x ♀H60
i.p.
B6♀
Naive
i.p.
FACS
D0
D40
B
PBL
Spleen
H60
H4
H7
Tet-PE
CD11a-FITC
B6 ♀
← H60♀
←Balb.B♂
B6 ♀
←Balb.B♂
B6 ♀
← H60♀
←BALB.B♂
B6 ♀
←BALB.B♂
% H60-Tet+ /CD8 T cells
% H4-Tet+ /CD8 T cells
% H7-Tet+ /CD8 T cells
ns
1°: ♀ H60 -
2°: ♂ Balb.B
C
H60
H28
H4
H7
H13
HY-UTY
VSV
F5NP
BALB.B ♂
B6 ♀
IFN-γ-PE
CD8-APC
B6 ♀
←Balb.B♂
B6 ♀
← H60♀
←Balb.B♂
D
H60
H4
H7
Tet-PE
CD11a-FITC
B6 ♀
← H60♀
←BALB.B♂
B6 ♀
←BALB.B♂
% H60-Tet+ /CD8 T cells
% H4-Tet+ /CD8 T cells
% H7-Tet+ /CD8 T cells
ns
1°: ♀ H60 -
2°: ♂ Balb.B
E
H60
H28
H4
H7
H13
HY-UTY
VSV
F5NP
BALB.B ♂
B6 ♀
IFN-γ-PE
CD8-APC
B6 ♀
←Balb.B♂
B6 ♀
← H60♀
←Balb.B♂

Figure 8. Immune hierarchy of minor histocompatibility antigens in H60-specifc tolerized mice .

(A) Female B6 mice that had been primed with female B6.CH60 spleen cells were i.p. injected with splenocytes from male BALB.B. (B) PBLs and splenocytes taken from the immunized mice on day 7 post-immunization were stained with H60- , H4-, or H7- tetramer PE in combination with APC-conjugated anti-CD8 mAb and FITC-conjugated anti-CD11a mAb for flow cytometry. Representative flow cytometry data obtained after gating on CD8 cells are shown, with percentages of tetramer binding CD8 T cells noted. (C) Splenocytes from mice immunized with BALB.B were prepared on day 7 after immunization and tested *ex vivo* for IFN-γ production after stimulation with peptides. The cells were intracellular stained APC-conjugated anti-IFN-γ mAb and FITC-conjugated anti-CD8 mAb. Representative flow cytometry data obtained after gating on CD8 cells are shown, with percentages of IFN-γ^+ CD8 T cells.

Reversion of immune hierarchy in H60-matched transplantation

Aforementioned results demonstrated that the absence of H60-specific CD8 T cell expansion, that is tolerance, in response to BALB.B stimulation caused concomitant suppression of subdominant Ag specific CD8 T cell expansions. Therefore, I investigated whether H60-matching between donor and host would also induce tolerance of CD8 T cell responses for subdominant antigens. I immunized B6.CH60 (MHC- and H60-matched with BALB.B) with male BALB.B spleen cells and the frequencies of H60-, H4- and H7 tetramer^{+} CD8 T cell were monitored by flow cytometric analysis (Fig. 9A). In contrast to the results obtained under H60-specific tolerized condition, it was shown that H4-tetramer-binding CD8 T cells detected at distinct levels in H60-matched H60 congenic mice after BALB.B immunization: 2.3% of CD8 T cells in blood and 3.4% of CD8 T cells in spleens (Fig.9B). In IFN-γ production assay, there were CD8 T cell producing IFN-γ in response to H4 peptide-stimulation in the H60 congenic as well as B6 mice after BALB.B immunization (Fig. 9C). These findings were also reproduced when the tetramer-binding and IFN-γ production analysis were done with in vitro amplified MLC cells (Fig.

9D,E). Thus, suppression of CD8 T cells to subdominant minor H antigens was a phenomenon specific to CD8 T cell response detected in mice where H60-specific CD8 T cell response was tolerized, not in the mice with H60-match.

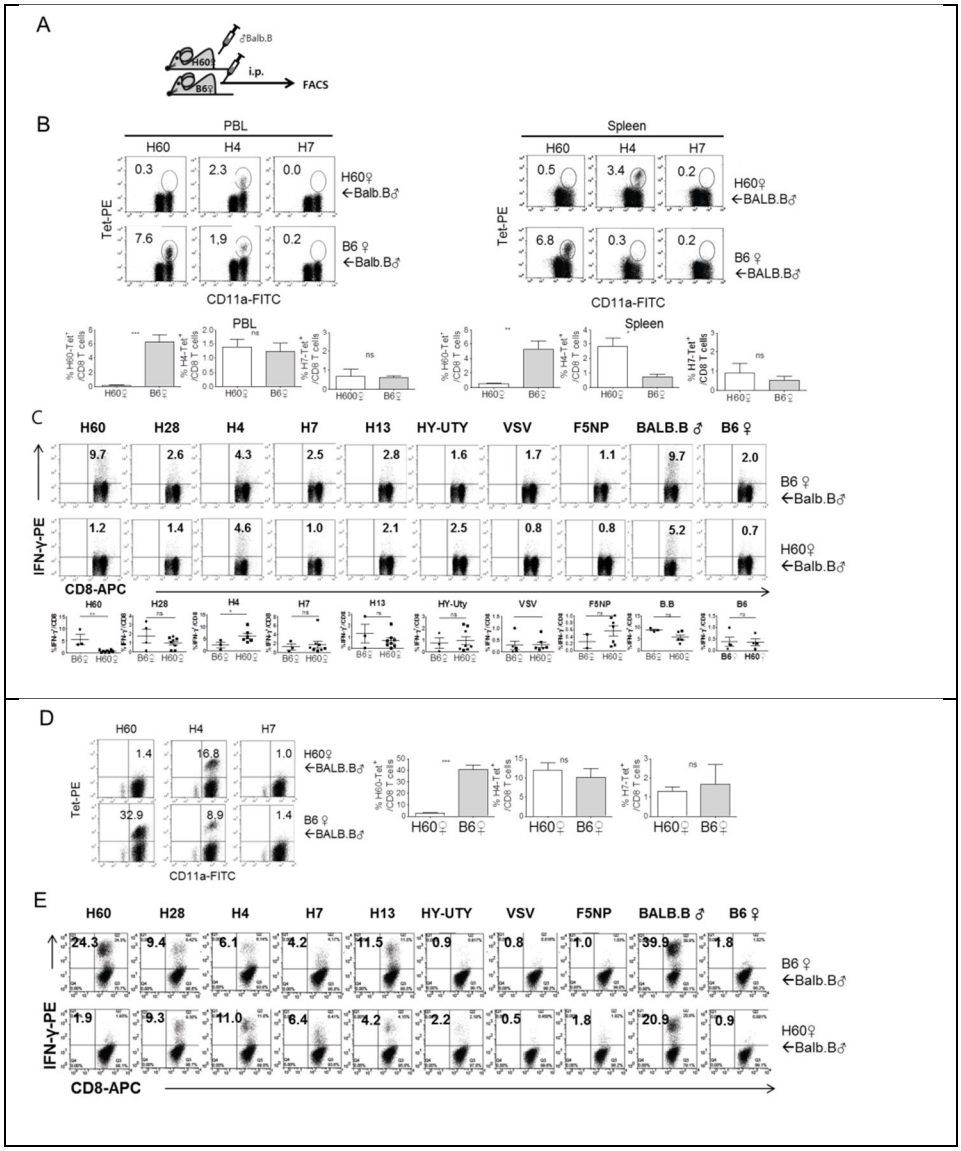
A
♂Balb.B
H60♀
i.p.
B6♀
FACS
B
PBL
Spleen
H60
H4
H7
Tet-PE
CD11a-FITC
H60♀ ←Balb.B♂
B6 ♀ ←Balb.B♂
H60♀ ←BALB.B♂
B6 ♀ ←BALB.B♂
C
H60
H28
H4
H7
H13
HY-UTY
VSV
F5NP
BALB.B ♂
B6 ♀
IFN-γ-PE
CD8-APC
B6 ♀ ←Balb.B♂
H60♀ ←Balb.B♂
D
H60♀ ←BALB.B♂
B6 ♀ ←BALB.B♂
E
B6 ♀ ←Balb.B♂
H60♀ ←Balb.B♂

Figure 9. Immune hierarchy of minor histocompatibility antigens in B6.CH60 (MHC− and H60 matched with BALB.B).

(A) Female B6.CH60 mice were i.p. injected with splenocytes from male BALB.B. (B) PBLs and Splenocytes taken from the immunized mice on day 7 post−immunization were stained with H60− , H4−, or H7− tetramer PE in combination with APC−conjugated anti−CD8 mAb and FITC−conjugated anti−CD11a mAb for flow cytometry. Representative flow cytometry data obtained after gating on CD8 cells are shown, with percentages of tetramer binding CD8 T cells noted. (C) Splenocytes from mice immunized with BALB.B were prepared on day 7 after immunization and tested *ex vivo* for IFN−γ production after stimulation with peptides. The cells were intracellularly stained with APC−conjugated anti−IFN−γ mAb and FITC−conjugated anti−CD8 mAb. Representative flow cytometry data obtained after gating on CD8 cells are shown, with percentages of IFN−γ^+ CD8 T cells.

Concomitant suppression of subdominant H4-specific CD8 T cell response in H60-tolerized mice requires co-expression of H60 and H4 in immunizing cells

Next, I questioned whether H4-specific CD8 T cell response would be suppressed in H60-tolerized mice. To address this question, I immunized B6 mice which had been tolerized against H60 with H4 congenic B6 splenocytes which do not express H60, and examined expansion of H4-specific CD8 T cells in response to the stimulation. Immunization with BALB.B splenocytes was done in parallel. While the H4-tetramer-binding CD8 T cells were not detected in H60-tolerized mice after BALB.B splenocytes immunization, they were detected in the H60-tolerized mice after H4 splenocytes immunization (Fig.10) Therefore, the suppression of CD8 T cell response to subdominant H4 was not due to tolerance of bystander CD8 T cells reactive to H4, but was related with immune-competition among CD8 T cell with different specifies.

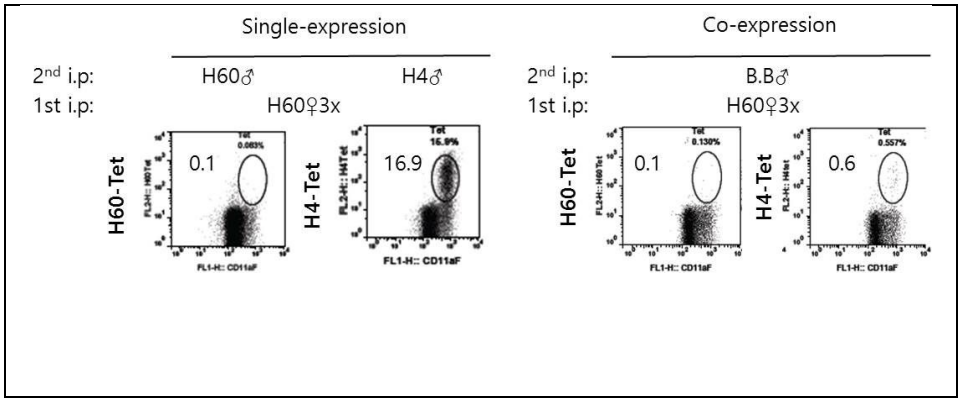

Figure 10. Concomitant suppression of subdominant H4-specific CD8 T cell response in H60-tolerized mice requires co-expression of H60 and H4 in immunizing cells.

(A) Female B6 mice that had been primed with female B6.CH60 spleen cells were i.p. injected with splenocytes from male BALB.B, B6.CH60, or B6.CH4. PBLs taken from the immunized mice on day 7 post-immunization were stained with H4- or H4- tetramer PE in combination with APC- conjugated anti-CD8 mAb and FITC-conjugated anti-CD11a mAb for flow cytometry. Representative flow cytometry data obtained after gating on CD8 cells are shown, with percentages of tetramer binding CD8 T cells noted.

DISCUSSION

Previous studies have shown that CD4 T cell help is an important factor on the quantity and quality of CD8 T cell response. In accordance with the previous studies, this study demonstrated that memory expansion of CD8 T cells were impaired when the CD8 T cells were primed in the absence of CD4 help and the help-deficiency induced CD8 T cell memory impairment was reproduced with different immunization methods. Interestingly, I also revealed that the help-deficiency during the priming of antigen-specific CD8 T cells not only implemented the memory impairment, that is, tolerance to antigen-re-exposure, but also tolerance environment in the immunized hosts.

In the previous study, the memory impairment of CD8 T cells activated in the absence of CD4 help were equivalent to CD8 T cell exhaustion [23]. And the exhaustion of CD8 T cells was due to inefficient antigen-clearance which led to antigen-persistence in the immunized hosts. Therefore, enforced early clearance of antigen could render the help-deficient CD8 T cells to generate memory cells, indicating that the CD4 help is not the factor determining the memory generation from

activated CD8 T cells. In addition to this, I demonstrated that tolerance environment has been established in the host that was primed under help-deficient condition, as evidenced by the lack of expansion of naïve H60-specific CD8 T cells that were adoptively transferred into the help-deficient primed hosts. The tolerance environment exerted suppressive effects on the CD8 T cells specific for other subdominant minor H antigens, resulting in the reduced immunity against BALB.B transplanted cells. However, CD8 T cell expansion against subdominant H4 minor was significantly enhanced after BALB.B cell transplantation into H60 congenic mice, in which case H60-specific CD8 T cells was not activated, either, maintaining the similar intensity of immunity against BALB.B cells. These results indicate that lack of expansion of H60-specific CD8 T cells does not always guarantee the tolerance effect on anti-BALB.B immunity. The tolerance effect on anti-BALB.B immunity could be observed only when the H60-specific CD8 T cells were tolerized, or impaired for memory expansion. The tolerance effect was dependent on the presence of H60 expression in association with expression of other minor H antigens by the immunizing cells, BALB.B. Based upon these

results, I suggest that the tolerance effect observed in the hosts primed against H60 under help-deficient condition may rely on the active suppression of CD8 T cell immunity against subdominant minor H antigens by exhausted H60-specific CD8 T cells or the suppressive activity may be exerted by non-CD8 T cell compartments in the hosts. Cellular mechanism underlying the phenomenon of tolerance in the help-deficient primed hosts remains to be identified.

Cell-based antigens are considered to be noninflammatory and induce CD8 T-cell response in a CD4 help-dependent manner, requiring the presence of CD4 help for primary expansion of the specific CD8 T cells. This study provides insight into how CD4 help and CD8 T-cell immunity can be used to design strategies to enhance CD8 T-cell memory for antitumor immunity or to promote transplantation tolerance.

CHAPTER 2

The effect of single amino acid variation on development of H60-reactive CD8 T cell response

INTRODUCTION

Minor histocompatibility antigens are peptide fragments naturally processed from polymorphic proteins that generate epitope presented by MHC [24]. After MHC-matched allogeneic transplantation, allogeneic minor H antigens are recognized as foreign antigens by CD4 and CD8 T cells, resulting in graft rejection

H60 is a hematopoietic cell-specific dominant minor histocompatibility antigen that is considered a target antigen for modeling tumor therapy that enhances the graft-versus-leukemia (GVL) effect while suppressing graft-versus-host disease (GVHD) [15, 25]. Therefore, the characterization of the immune response to minor H antigen, H60, and the identification of the T-cell receptor (TCR) repertoires during the H60 specific CD8 T cell responses are necessary to facilitate the development of treatments that enhance GVL and suppress GVHD.

The H60 specific CD8 T cell response is CD4 dependent both in induction of the primary response and in expansion of memory cells [16]. The CD4 help through the cognate

recognition of antigen-presenting cells by CD4 and CD8 T cells is mediated via an interaction between CD40 and CD40L [16].

In the presence of CD4 help, the large repertoire of T cells recruited to the H60specific response include Vβ4, Vβ5, Vβ8, and Vβ11 [12]. Spectratyping analysis has demonstrated that the various Vβ the inclusion of families participate in the H60-specific primary, secondary, and tertiary response and CDR3 length diversity within each Vβ subfamily gradually decreases with repeated response induction [17].

MHC I molecules bind peptides that are 8-10 amino acid in length [26]. In octameric peptides displayed by H2-Kb, residues at P2, P3, P5, and P8 contact with the MHC I molecule and residues at P1, P4, P6, and P7 potentially accessible to the TCR [27, 28]. Peptides modified based on amino acid substitutions are termed "altered peptide ligands" (APLs) [29]. Such APLs can generate qualitatively different T cell responses compared with those produced by the antigenic peptide [30, 31]. Previous studies have shown that weak interactions of the T cell receptor (TCR) with self-peptide-MHC complexes are required to protect thymocytes from death by neglect and to promote the positive selection of naïve T cells

in thymus [32]. In contrast, strong interactions cause negative selection by apoptosis in thymus, when high affinity ligands are presented endogenously by cortical epithelial cells [33]. The strength of interaction between TCR and self-peptide-MHC complexes also regulates autoreactive T cell response in periphery.

Octapeptide LTFNYRNL derived from H60 presented by the Kb MHCI molecules. In a B6 anti BALB.B setting, the H60 specific CD8 T cell receptor recognizes the LTFNYRNL/H2-K^b, resulting in the induction of H60-specific CD8 T cell responses. Since the B6 mouse strain does not express H60, precursor of H60-specific CD8 T cells have survival benefits on negative selection and precursor is higher than other minor H antigen-specific CD8 T cells [14, 15], but this lacks direct supporting evidence. In addition, no investigations into positive thymic selection of H60-specific CD8 T cells using altered peptide ligands that mimic self-protein have been reported. Experiments using altered H60 peptide ligands might be helpful in understanding the thymic selection process for H60-specific CD8 T cells and in controlling the specific response. To address these issues, I generated a transgenic mouse expressing a

single-amino-acid variant of H60, designated H60H, and analyzed its immunogenicity and the composition of the TCR repertoire it recruits to the specific CD8 T-cell response. Because position 4 (p4) of the H60 epitope is thought to be important for the TCR interaction, I elected to replace the naturally occurring arginine residue at p4 with histidine, thereby creating the H60 variant H60H, based on peptide screening with a cytotoxicity assay. Using splenocytes from H60H transgenic (H60H Tg) mice, I induced the CD8 T-cell response in B6 mice and compared the immune kinetics and the diversity of the responding TCRs with those for the natural H60 epitope (hereafter, H60N). These results demonstrate that H60H could be used as an immunogenic epitope that recruits diverse TCRs to the specific response. In addition, I identified some overlap in TCR usage between CD8 T cells responding to H60H vs. H60N stimulation, suggesting that the H60H Tg mouse will be useful for understanding the selection process and control of CD8 T cells specific for H60.

MATERIALS AND METHODS

1. Mice

C57BL/6 mice from Jackson laboratory (USA) were used for immunization. Transgenic mice expressing the H60H variant (H60H Tg mice) were obtained by micro injecting DNA into the fertilized eggs of B6 mice. The injected DNA contained a complete but altered, FLAG-tagged, H60 cDNA sequence under control of the chicken β-actin promoter and a cytomegalovirus enhancer; the altered sequence encoded an asparagine (N) → histidine (H) substitution at p4 of the epitope sequence. The H60H Tg mice were maintained at Jackson Laboratory or at the Bio medical Center for Animal Resource Development of Seoul National University College of Medicine in Korea, as were B6.C-H60^{c}/DCR mice and H60 transgenic (H60N Tg) mice expressing H60 protein under the control of the chicken β-actin promoter [34]. Male F1 hybrid mice are the offspring of a cross between H60H Tg females and C.B10-H2^{b}/LiMcdj (BALB.B: H-2^{b}) males. The F1 hybrid mice were maintained or at the Bio medical Center for Animal Resource Development of Seoul National University College of Medicine in Korea.

2. Immunization

To induce a specific CD8 T-cell response, splenocytes (2×10^7 cells) from H60N Tg, H60H Tg or F1 hybrid mice were injected intraperitoneally into female B6 mice or H60H Tg. A secondary response was induced by intraperitoneally injection of the splenocytes into B6 mice 30-50 days after primary immunization.

3. *In vitro* cytotoxicity assay

Splenocytes isolated from B6 mice was labeled with 2.5 μM CFSE (Invitrogen). A total of 5×10^6 spleen cells labeled with CFSE were incubated with altered peptide ligands at the concentrations indicated for 1h at 37. After washing 2 times to remove free peptide, 1×10^5 H60 specific CTLs (1:1) were added. Then, the mixtures (1:1) of target cells and CTLs were incubated for 4h. Flow cytometry was performed to analyze cytotoxicity of CTLs and detect the CFSE-labeled target cells.

Mixed lymphocyte culture

Splenocytes (2.5×10^7) from immunized mice were cultured with 3.5×10^7 irradiated H60N Tg splenocytes in 10ml culture

media for 7 days in the presence of 50U/ml IL-2. CD8 effector cells from the mixed lymphocyte culture (MLC) were tested for cytotoxicity and flow cytometry

In *vitro* IFN-γ production assay

Splenocytes harvest from immunized mice on day 7 post-boosting were after in vitro stimulation with peptides, fixed, and permeabilized for staining with anti-IFN-γ Ab and subsequent flow cytometric analysis.

Antibodies and flow cytometry

For low cytometry, peripheral blood lymphocytes (PBLs) remaining after red blood cell lysis or splenocytes were stained with H60H- or H60N-tetramer-PE in addition to FITC-conjugated CD11a Ab (M17/4; eBioscience) and APC-conjugated anti-mouise CD8 mAb (53-6.7;eBioscience). Vβ analysis was performed by staining splenocytes with PE-conjugated H60H or H60N tetramers, APC-conjugated anti-mouse CD8 mAb, and FITC-conjugated anti- Vβ mAbs. The Abs used for Vβ typing were purchased from BD pharmingen as follows: Vβ(B06), Vβ3.1 (KJ25), Vβ4 (KT4), Vβ5.1/5.2

(MR9-4), Vβ6 (RR4-7), Vβ7 (TR310), Vβ8.1/8.2 (MR5-2), Vβ8.3 (1B3.3), Vβ9 (MR10-2), Vβ10 (B21.5), Vβ11 (RR3-15), Vβ12 (MR11-1), Vβ13 (MR12-3), Vβ14 (14-2), and Vβ17 (KJ23).

Statistical analysis.

Statistical analysis was performed using GraphPad Prism (version 5, GraphPad Software, La Jolla, CA, USA). All error bars represent the standard error of the mean (SEM). P values were determined by Student's t-tests. (Unpaired two-tailed: $*P < 0.05$, $**P < 0.01$, $***P < 0.001$)

.

RESULTS

Some H60N specific CD8 T cells have cross-reactivity to altered peptide ligand, H60H

To understand the role of single amino acid variation in thymic selection of H60-reactive CD8 T cells and the mechanism of dominance of the H60-specific CD8 T cell response, I investigated the sensitivity of H60 CTLs to various altered peptide ligands. I observed that H60 CTLs partially have cytotoxicity for H60H (LTFHYRNL) and H60Q (LTFQYRNL) compared with the wild type H60 peptide (H60N) (Fig. 1A). In addition, The H60H tetramer-binding CD8 T cells were detected in up to 10% of the H60 CTLs (Fig. 1B). These observations implied that some H60 CTLs have cross-reactivity to APL, H60H.

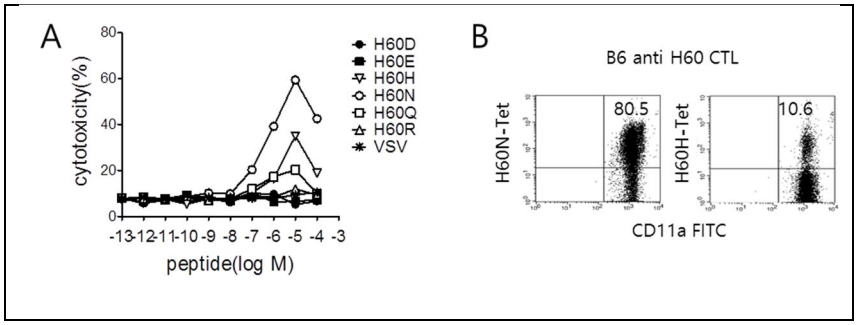

Figure 1. Cytotoxicity of H60N-specific CD8 T cells for altered peptide ligands of H60.

(A) For target cells, B6 splenocytes labeled 2.5 μM CFSE were pulsed with altered peptide ligand of H60N. The mixtures (1:1) of target cells and CTLs were incubated for 4h. Flow cytometry was performed to analyze cytotoxicity of CTLs and detect the CFSE-labeled target cells. (B) Established H60 CTLs were stained with H60N- or H60H-tetramer-PE in combination with APC-conjugated anti-CD8 mAb and FITC-conjugated anti-CD11a mAb for flow cytometry. Representative flow cytometry data obtained after gating on CD8 cells are shown, with percentages of tetramer binding CD8 T cells noted.

.

Induction of an H60H-specific CD8 T-cell response and detection of the cross-reactive population

To generate a transgenic mouse expressing a single-amino acid variant of H60 (H60H) in a B6 background, a DNA fragment containing an altered, FLAG-tagged, full-length H60H cDNA sequence under control of the chicken β-actin promoter was microinjected into B6 mouse eggs. The altered cDNA encoded an asparagine (N) → histidine (H) substitution at p4 of the CD8 epitope, changing the sequence from LTFNYLN(H60N) to LTFHYLN (H60H). Three lines of transgenic mice with PBLs positive for genomic DNA by PCR screening were obtained. One line was selected for further use because it yielded an H60H reverse transcription (RT)-PCR band comparable in density to the H60N band obtained from H60C mouse PBLs (data not shown). The splenocytes from this line, designated H60H Tg, were used as cell-based immunogens for the induction of the H60H-specific CD8 T-cell response via i.p. injection into B6 mice.

To examine the expression and immunogenicity of the H60H transgenic protein, I immunized five female B6 mice with

splenocytes from a male H60H Tg mouse and assessed them for the development of an H60H-specific CD8 T-cell response. As controls, female B6 mice were immunized with splenocytes from male H60 congenic mice or from male H60N Tg mice, which express the native H60 protein under control of the β-actin promoter [34]. PBLs periodically collected from the immunized B6 mice of each group were stained with H60N or H60H tetramers and analyzed by flow cytometry to detect H60N- or H60H-reactive CD8 T cells (Fig. 2). The flow cytometry results confirmed that H60H tetramer-binding CD8 T cells were present in the blood of B6 mice immunized with male H60H Tg mouse splenocytes. The peak frequency was observed on day 10 post-immunization, when 8% to 14% of the CD8 T cells were H60H tetramer-binding cells (Fig. 2A). The peak values were very similar to those obtained for H60N tetramer-binding CD8 T cells detected in the blood of B6 mice immunized with male H60N Tg or H60C mouse splenocytes. The overall kinetics of the H60H-specific CD8 T-cell response was similar to that of the H60-specific response induced by immunization with male H60N Tg or H60C mouse splenocytes (Fig. 2C). These observations confirmed the

expression of the H60H transgene and ability of the LTFHYLN variant peptide to act as an epitope, inducing a readily detectable level of CD8 T cell response. H60H or H60N tetramer-binding CD8 T cells were not detected in the blood from female B6 mice immunized with splenocytes from female H60H Tg, H60N Tg, or H60 congenic splenocytes (Fig. 2B). In this case, the lack of an H60H- or H60N specific CD8 T-cell response was attributable to the lack of a CD4 T-cell response, which requires the recognition of the HY-Dby epitope originating from the male H60H splenocyte. This help-dependence is characteristic of the CD8 T-cell response to a non-inflammatory cellular antigen. Therefore, in subsequent experiments, only splenocytes originating from male mice were used for immunization.

These results demonstrated that splenocytes from H60H Tg mice provide a new cell-based CD8 epitope. Furthermore, they showed that the H60H epitope is as immunogenic as the natural H60N epitope originating on splenocytes of H60N Tg or H60C mice.

I next examined whether i.p. injection of H60H Tg splenocytes would induce a memory response in female B6

mice previously challenged with the same splenocytes. Using flow cytometry, I examined the PBLs of H60H Tg splenocyte immunized mice after re-challenge with H60H Tg splenocytes (Fig. 2D) to determine the kinetics of the memory response (Fig. 2E). I compared this kinetics with that of the H60-specific memory response induced by secondary challenge with H60N Tg or H60C mouse splenocytes. A comparative plot of the frequencies of peripheral blood CD8 T cells positive for H60H or H60N tetramer staining over time demonstrated that rechallenge with splenocytes from H60H Tg mice induced a specific memory CD8 T-cell response (Fig. 2D, left panel), just as re-challenge with splenocytes from H60N Tg or H60C mice induced a specific memory response (Fig. 2D, middle and right panels). The peak frequencies (50-70% of CD8 T cells in blood) were observed on day 7 post-secondary immunization and were 5 times higher than the peak frequencies after primary challenge in all three cases (Figs. 2D and 2E).

During the investigation of the H60H-specific memory response, I noticed that some CD8 T cells in blood from H60H splenocyte re-challenged mice were positive for H60N tetramer staining (4.1% of peripheral blood CD8 T cells; Fig.

2C, lower left panel). The reverse was also true: H60H tetramer-binding CD8 T cells were detected in up to 3% of the peripheral blood CD8 T cells from H60N splenocyte re-challenged mice (Fig. 2D, upper middle panel). These observations implied that some CD8 T cells from the H60H- or H60-specific responses were cross-reactive but were not detected until after expansion during the memory response. This finding suggested overlap in the TCR usage of CD8 T cells responding to H60H and H60N.

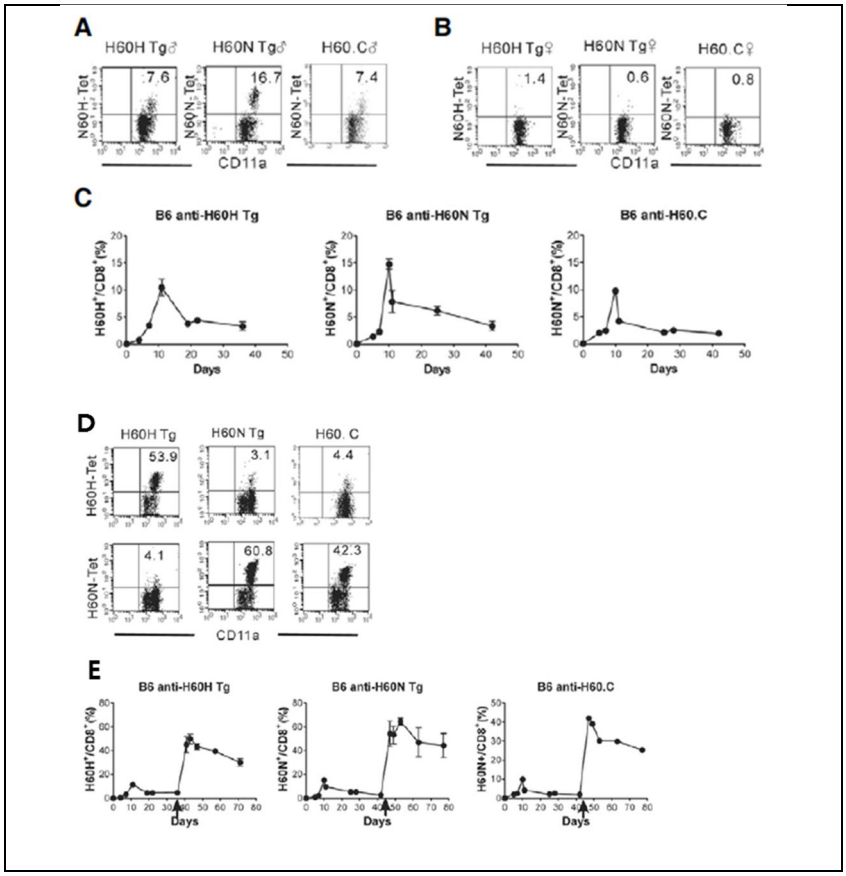

Figure 2. Flow cytometric evaluation of the H60H-specific CD8 T-cell response.

(A) Female B6 mice were i.p. injected with splenocytes from male (A) or female (B) H60H Tg, H60N Tg, or H60C mice. PBLs taken from the immunized mice on day 10 post-immunization were stained with H60H or H60N tetramer-PE in combination with APC-conjugated anti-CD8 mAb and FITC-conjugated anti-CD11a mAb for flow cytometry. Representative flow cytometry data obtained after gating on

CD8 cells are shown, with percentages of H60H or H60N tetramer-binding CD8 T cells noted. (C) Female B6 mice were i.p. injected with splenocytes from male H60H Tg (left), H60N Tg (center), or H60C (right) mice. PBLs were taken from the immunized mice at the indicated number of days post-immunization, stained, and analyzed by flow cytometry as in (A) and (B) for the percentages of H60H or H60N tetramer-binding CD8 T cells. (D) Female B6 mice were immunized with splenocytes from male H60H Tg (left panels), H60N Tg (center panels), or H60C (right panels) mice and re-challenged 30-50 days later to induce a secondary response. PBLs taken from the immunized mice were stained with H60H or H60N tetramer-PE in combination with APC-conjugated anti-CD8 mAb and FITC-conjugated anti-CD11a mAb for flow cytometric analysis. (D) Representative flow cytometry data for PBLs taken from the immunized mice on day 7 post-secondary immunization are shown, with percentages of tetramer-binding CD8 T cells noted. (E) PBLs were taken from the immunized mice at the indicated days after primary challenge, stained, and analyzed by flow cytometry for the percentages of tetramer-binding CD8 T cells as in (D). The

day of re-challenge is indicated by an arrow. Data shown are representative of at least three independent experiments.

Diverse Vβ families respond to H60H stimulation

The ready detectability of H60H tetramer-binding CD8 T cells in blood during the H60H-specific primary response suggested that either a broad repertoire of T cells with diverse TCRs or a narrow repertoire of T cells with repeated TCRs was involved in the response. Therefore, I examined whether the TCR repertoire participating in the H60H-specific response was as wide as that participating in the response to the natural H60 epitope. In particular, the detection of a minor population of crossreactive CD8 T cells (Fig. 2D) prompted me to search for overlap in TCR usage for the two responses.

First, I investigated the usage of TCR Vβ regions. Splenocytes from female B6 mice challenged with H60H Tg splenocytes were prepared on day 10 post-immunization, and stained with H60H tetramers and Abs against specific Vβ regions and CD8 for flow cytometry analysis. Splenocytes from female B6 mice immunized with H60N Tg splenocytes were similarly prepared and stained with H60N tetramers and Vβ and CD8 Abs for comparison. The flow cytometry analysis showed that the H60H tetramer-positive cells included various Vβ families(Fig. 3A, upper row) and that the diversity of Vβ

families participating in the H60H-specific and H60N-specific CD8 T-cell responses was comparable (Fig. 3A, compare both rows). Plotting of the frequencies of occurrence of each Vβ family in the H60H or H60N tetramer-binding CD8 T cells revealed a considerable difference in Vβ usage (Fig. 3B). While Vβ4, Vβ5.1/2, Vβ8, and Vβ11 were dominant families in both the H60H- and H60N-specific CD8 T cells, Vβ6, Vβ7, Vβ14, and Vβ17 were also dominant families in the H60H-specific cells, but Vβ2, Vβ10, and Vβ13 were dominant families in the H60N-specific cells. Since Vβ4, Vβ5.1/5.2, Vβ8, and Vβ11 are frequently used during the H60-specific CD8 T cell response induced by the injection of H60C splenocytes into female B6 mice [17], they appear to be commonly used in the CD8 T-cell response to H60-related antigens. Together, These Vβ analysis demonstrates that diverse Vβ families are recruited in the H60H-specific CD8 T-cell response.

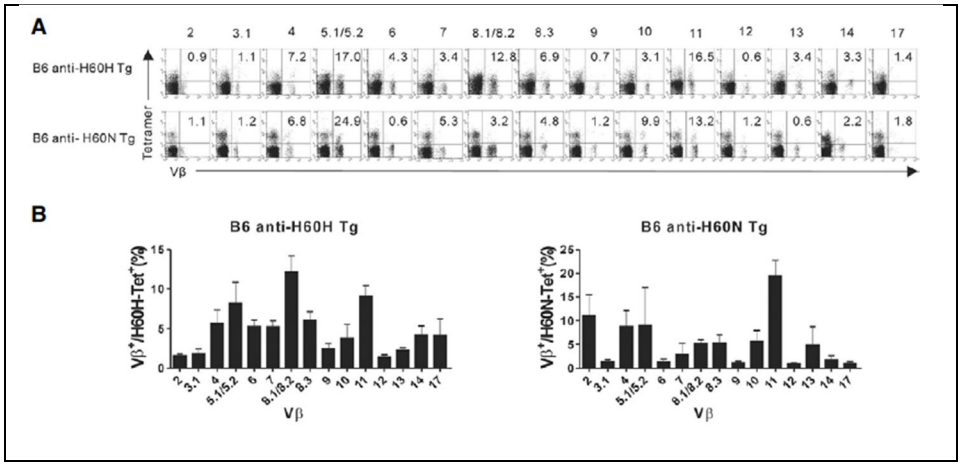

Figure 3. Vβ analysis of CD8 T cells involved in the H60H-specific response.

(A) Ten days after female B6 mice were immunized with splenocytes from male H60H Tg (upper panels) or H60C (lower panels) mice, their splenocytes were harvested, stained with FITC-conjugated Vβ Abs in combination with APC-conjugated anti-CD8 mAb and PE-conjugated H60H (upper panels) or H60 (lower panels) tetramer-PE, and subjected to flow cytometry. Representative flow cytometry data are shown. Numbers above panels indicate the particular Vβ region analyzed, and numbers within panels indicate the percentages of H60H tetramer-binding (upper panels) or H60N tetramer-binding (lower panels) CD8 T cells positive for the indicated Vβ region. (B) Mean percentages of H60H (left) or H60N

(right) tetramer-binding CD8 T cells that were also positive for the indicated Vβ regions. Each data point shown represents the mean ± S.E.M. for 3 immunized mice.

Clonotypic diversity of H60H-specific CD8 T cells and minor overlap in TCR usage with H60N-specific CD8 T cells

The observed commonality of certain Vβ families to H60H- and H60N-specific CD8 T cells raised the issue of possible overlaps at the clonotypic level. To compare the CD8 T-cell clonotypes, I sequenced the Vβ CDR3 regions of Vβ4, Vβ8.3, and Vβ11-positive CD8 T cells. Using magnetic cell separation, I purified H60H tetramer-binding CD8 T cells from the splenocytes of H60H Tg splenocyte-immunized mice on day 10 post-immunization and extracted the total RNA. After cDNA synthesis with a Cβ primer, the cDNA was subjected to RT-PCR with a Cβ 3′ primer and Vβ-specific 5′ primers. The RT-PCR products were subcloned into the pGEM-T vector and transformed into E. coli. More than 100 different transformant colonies were picked and processed for sequencing of the Vβ CDR3 region, and all in-frame CDR3 sequences were selected. As a result, unique clonotypes were identified for each Vβ. Of the 78 bacterial colonies with in-frame Vβ4 sequences from H60H-specific CD8 T cells, 17 unique Vβ4 clonotypes were identified (Table 1): the CDR sequence

ASSQDRVANTEVFFGKGTRLTVVE was the most frequent clonotype (Fig. 4A). Of the 48 bacterial colonies with in-frame Vβ4 sequences from H60N-specific CD8 T cells, 7 unique Vβ4 clonotypes were identified, but none overlapped with those from H60H-specific CD8 T cells. Similarly, for H60Hand H60-specific CD8 T cells, I identified 36 and 15 unique Vβ8.3 clonotypes, respectively (out of 105 and 38 respective inframe Vβ8.3 sequences), but none of the clonotypes overlapped between the two responses (Fig. 4B).

In Vβ11 family, I identified 19 and 22 unique clonotypes for the H60H- and H60-specific CD8 T cell responses, respectively (out of 43 and 75 respective in-frame sequences). Eleven of these clonotypes were common to both responses, suggesting that these common clonotypes might be responsible for the observed cross-reactivity between the H60H and H60N epitopes (Fig. 4C). The CDR sequence ASSPETLERLFFGHGTKLSVE was the most frequently used CDR sequence in H60Hspecific CD8 T cells and the second most frequently used CDR sequence in H60-specific CD8 T cells (Fig. 4C). This clonotyping analysis demonstrated that the H60H- and H60N-specific CD8 T cell responses recruited

diverse clones within each Vβ family, and that most of the clonotypes were response-specific. However, some Vβ11 clones were shared by H60H- and H60-specific CD8 T cells. These results suggest that a single amino acid variation in epitope sequence can change the array of recruited CD8 T cell clonotypes and that a minor population of clonotypes may be common to response to both the original and altered epitope sequence.

Table 1. Clonotype analysis of some Vβ regions participating in H60H- or H60N-specific CD8 T-cell responses

Vβ region	B6 anti-H60H		B6 anti-H60N	
	In-frame CDR3 sequences	Unique CDR3 sequences (% of total)	In-frame CDR3 sequences	Unique CDR3 sequences (% of total)
Vβ4	78	17 (21.8%)	48	7 (14.6%)
Vβ8.3	105	36 (34.2%)	38	15 (39.5%)
Vβ11	43	19 (44.2%)	75	22 (29.3%)

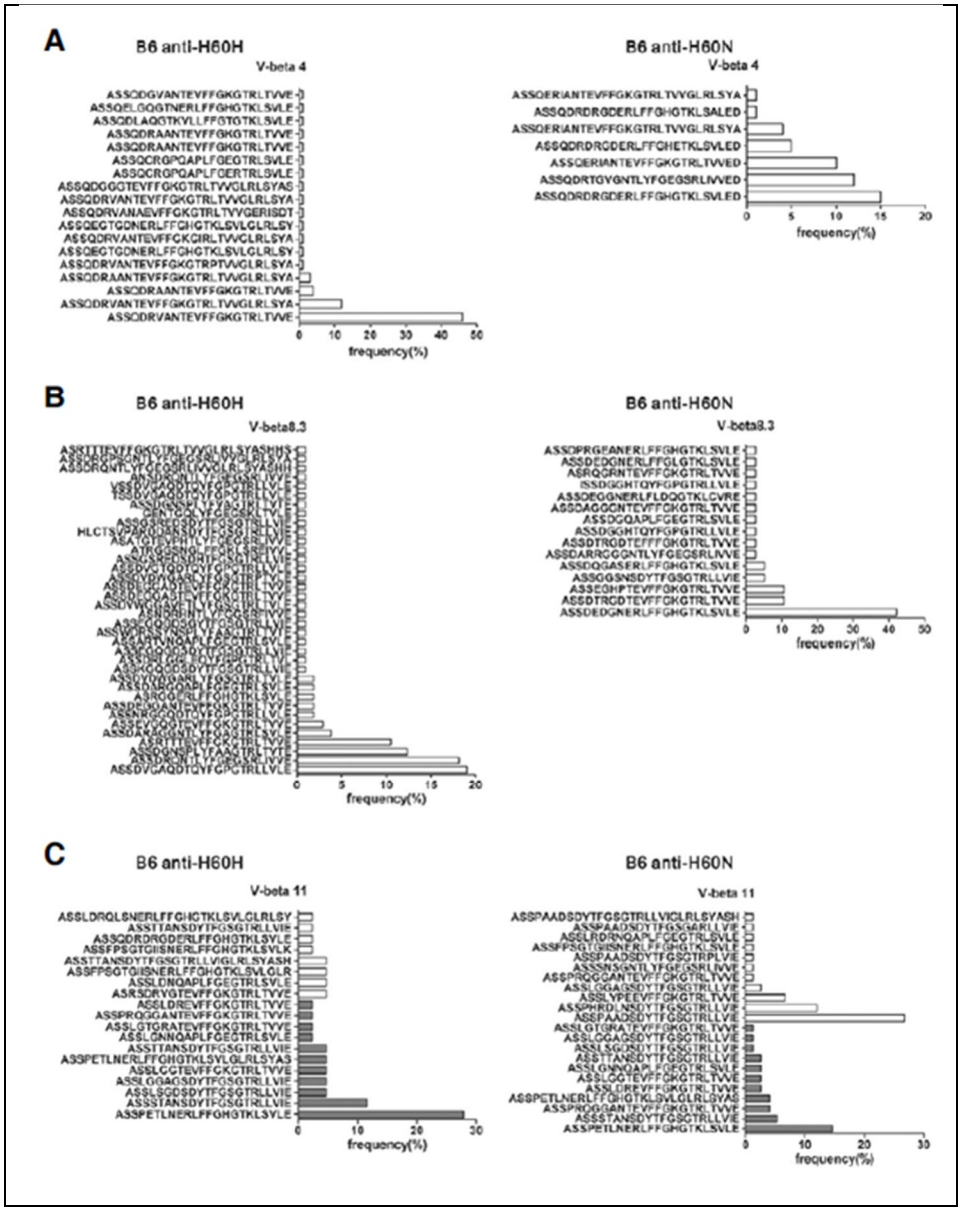

Figure 4. Clonotypic analysis of H60Hspecific CD8 T cells. Ten days after immunization of B6 mice with male H60H Tg or H60N splenocytes, their H60H tetramer-binding(for H60H-immunized mice) or H60N tetramer-binding (for

H60Nimmunized mice) CD8 T cells were purified by magnetic cell separation. Total RNA extracted from the purified cells was processed for cDNA synthesis, and the synthesized cDNA was amplified by PCR using Cβ2 3′ primer and Vβ4−, Vβ8.3−, or Vβ11−specific 5′ primers (A, B, and C, respectively). The RTPCR products were subcloned into the pGEM−T vector and sequenced to obtain the predicted amino acid sequences of the Vβ4 (A), Vβ8.3 (B), or Vβ11 (C) CDR3 regions. More than 100 different bacterial transformant colonies were processed for sequencing for each Vβ region. Each unique CDR3 sequence identified in H60H−specific (left panels) or H60N−specific (right panels) CD8 T cells is shown, together with its frequency of occurrence among all the colonies with inframe CDR3 sequences. Gray bars in (C) correspond to those Vβ11 clonotypes found in both H60H−specific and H60N−CD8 T cells.

H60N and H60H induce co-dominant CD8 T cell response in a B6 anti-BALB.B×H60H F1 hybrid.

I identified some population of H60 CTLs are cross-reactive on H60H sharing the same TCR (Fig.1). The results raised the possibility that the specific CD8 T-cell response to the H60H dominates over the responses specific other minor H antigen, competing between H60N and H60H recognized by same T cells. To determine whether this phenomenon could occur, I examined CD8 T cell response in a B6 anti BALB.BxH60H F1 that co-express H60N and H60H. The peak frequency was observed on day 7 post-immunization, when 2% to 3% of the CD8 T cells were H60H tetramer binding cells (Fig. 5A). The peak values were very similar to those obtained for H60N tetramer-binding CD8 T cells detected in the blood of same mice.

Next, I confirmed the hierarchy of the CD8 response to minor H antigens in a functional aspect. Splenocytes from the mice immunized were tested *ex vivo* for IFN-γ production in response to minor H antigen peptides. Intracytoplasmic staining for IFN-γ production demonstrated that CD8 T-cell response to the H60H dominant over the responses specific other minor

H antigen as H60N (Fig. 5B). Data suggests that H60N and H60H induce co-dominant CD8 T cell response, though they compete for recognize by same TCRs.

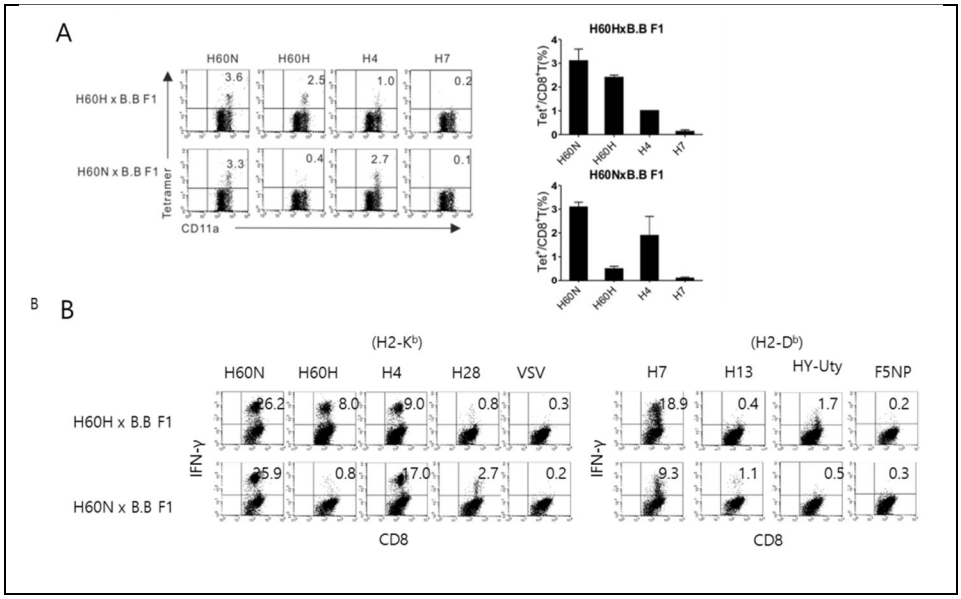

Figure 5. Immune hierarchy of H60N and H60H in a B6 anti-BALB.B × H60H F1.

(A) Female B6 mice were i.p. injected with splenocytes from BALB.B × H60H F1 or BALB.B × H60N F1 male mice. (A) PBLs taken from the immunized mice on day 7 post-immunization were stained with H60N- , H60H-, H4-, or H7- tetramer PE in combination with APC- conjugated anti-CD8 mAb and FITC-conjugated anti-CD11a mAb for flow cytometry. Representative flow cytometry data obtained after gating on CD8 cells are shown, with percentages of tetramer binding CD8 T cells noted. (B) Splenocytes from mice immunized with F1 hybrid cells were prepared on day 7 after immunization and

tested *ex vivo* for IFN-γ production after stimulation with peptides. The cells were intracellularly stained with APC-conjugated anti-IFN-γ mAb and FITC-conjugated anti-CD8 mAb. Representative flow cytometry data obtained after gating on CD8 cells are shown, with percentages of IFN-γ^+ CD8 T cells.

H60N induced CD8 T cell responses are reduced in H60H-Tg mice expressing H60H as a self-peptide during helpless primary response.

TCR cross-reactivity on self-peptide homologs plays some role in determining the size of MHCII-bound foreign peptide-specific $CD4^+$ T cell population [35]. The earlier work indicated that small foreign antigen specific naïve populations have lost cells with the highest-affinity TCRs due to deletion of clones that also recognize self-peptide ligands [35] [36] [37].

Based on the aforementioned results, I hypothesized that H60H would induce positive or negative selection of H60 specific CD8 T cells in thymus. To address this hypothesis, I examined whether cross-reactive population was eliminated in H60H-Tg mice that express H60H as a self-peptide under the control of the actin promoter. Indeed, as shown in Figure 4A, CD8 T cells in H60H-Tg mice bound H60H tetramer as well as H60N tetramer less than the comparable population in B6 mice during CD4 helpless response (Fig. 6B). In addition, CD8 T cell responses in H60H-Tg have lower affinity population of T cells specific for H60N (Fig. 6B). This difference was not observed in CD4 helped conditions (Fig. 6A), indicating that CD4 helpless

conditions are more induced cross-reactive population than CD4 help conditions.

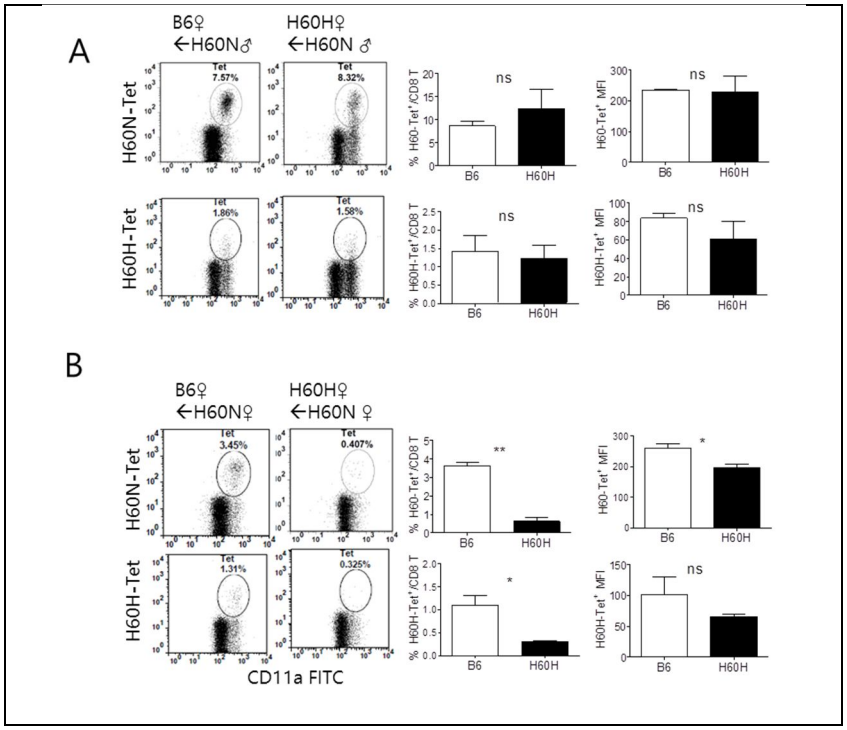

Figure 6. H60N induced CD8 T cell responses in H60H-Tg mice expressing H60H as a self-peptide.

(A, B) Female B6 or H60H-Tg mice were i.p. injected with splenocytes from male (A) or female H60N Tg mice (B). PBLs taken from the immunized mice on day 10 post-immunization were stained with H60N- or H60H-tetramer-PE in combination with APC-conjugated anti-CD8 mAb and FITC-conjugated anti-CD11a mAb for flow cytometry. Representative flow cytometry data obtained after gating on CD8 cells are shown, with and MFI and percentages of tetramer binding CD8 T cells noted.

H60N induced memory CD8 T cell responses are reduced in H60H-Tg mice expressing H60H as a self-peptide upon CD4 helpless condition because of clonal deletion.

The results raised the possibility that TCR cross-reactivity between self (H60H) and foreign (H60N) could lead reductions in the size of CD8 T-cell response because of non-selective expansion by clonal deletion but limited proliferation by CD4 helpless condition. To address this issue, I performed boosted mice in the resting memory stage with male H60N-Tg splenocytes (CD4 help), compared the peak burst sizes of the secondary responses. The peak frequency of both H60N-tetramer$^+$ cells and H60H-tetramer$^+$ cells during secondary response in H60H-Tg mice was similar to that obtained from B6 mice (Fig. 7A). In contrast, CD8 T cells in H60H-Tg mice bound H60H tetramer and H60N tetramer less than the comparable population in B6 mice during secondary response (Fig. 7B). These results indicate that H60-specific CD8 T cells populations have lost cells with cross-reactive TCRs due to deletion of clones that also recognize self-peptide ligands (H60H) upon CD4 helpless condition.

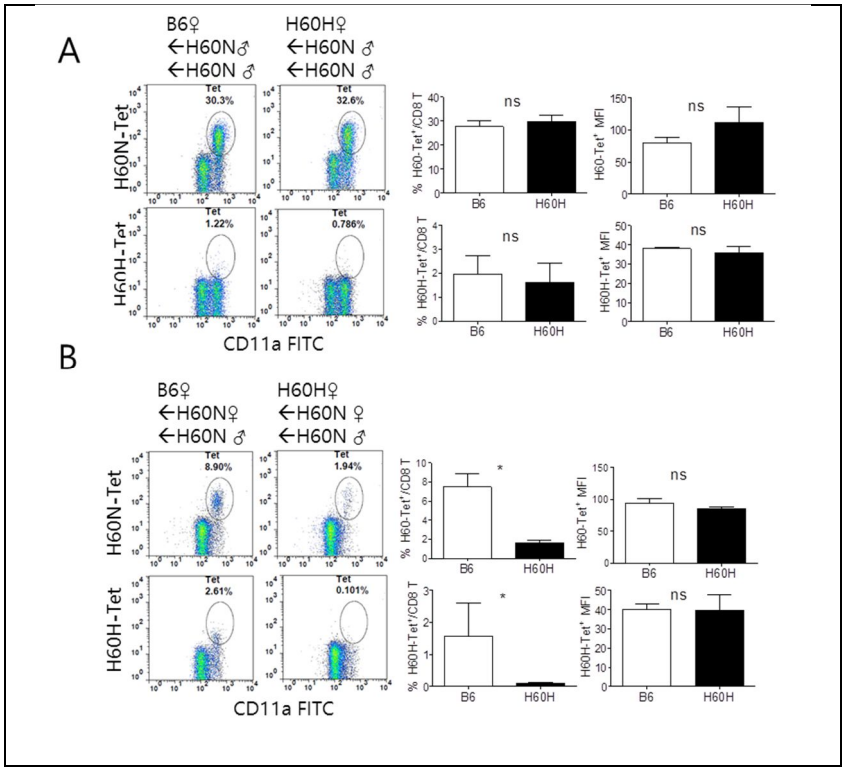

Figure 7. H60N induced memory CD8 T-cell response in H60H-Tg mice expressing H60H as a self-peptide.

Female B6 or H60H-Tg mice were i.p. injected with splenocytes from male (A) or female H60N Tg mice (B). Then, a secondary response was induced by i.p. of the H60N-Tg cells 30-50 days after primary immunization. PBLs taken from the immunized mice on day 7 post-immunization were stained with H60N- or H60H-tetramer-PE in combination with APC-conjugated anti-CD8 mAb and FITC-conjugated anti-CD11a mAb for flow cytometry. Representative flow cytometry data

obtained after gating on CD8 cells are shown with MFI and percentages of tetramer binding CD8 T cells noted.

. DISCUSSION

In this study, I demonstrated that H60H, a single-amino-acid variant of the natural H60 epitope, induces a CD8 T-cell response as strong as that induced by H60. The TCRs recruited to the H60H-specific and H60-specific CD8 T-cell responses were similarly diverse, suggesting that H60H is an immunodominant artificial protein. Researchers often use peptide derivatives or variants to modulate immune responses. Some alterations in peptide ligands can affect the Th1 versus Th2 nature of the response: peptides with a high MHC or TCR affinity skew the response towards the Th1 phenotype, whereas peptides with a low MHC or TCR affinity have the opposite effect [38]. Altered peptides have been used to alter the Th2 T-cell response to the immunodominant peptide in an infection model, raising the possibility that sequence derivatives might be used to prevent infection [39]. Various sequence derivatives have also been designed for use in therapeutic intervention in experimental autoimmune diseases [40]. Peptide modifications currently used for these purposes include not only changes in sequence but also post-translational modifications [41]. The characterization of a single-amino-

acid variant of H60 may provide basic knowledge needed for the development of measures to intervene in H60-related graft rejection or GVHD. Most studies of altered peptide ligands have focused on the effects of these ligands on the T cell response to the original peptide. I contend that the host immunity conferred by the variant itself has not been fully appreciated. An understanding of the mechanism of this immunity is important in elucidating the mechanism for modulation of the response to the original natural epitope. Therefore, in the present study, I characterized the immunologic response to an altered peptide (H60H) before examining the effect of the altered peptide on the response to the native peptide (H60N). H60H Tg spleen cells were found to provide a cell-based immunogenic epitope that induced a strong immune response in a CD4 help-dependent fashion. The broad diversity of the TCR repertoire recruited in the H60H-specific response suggests a potential for deviation between the H60H- and H60N-specific responses. The partial overlap in TCR usage between H60H- and H60N-specific CD8 T cells increases the probability that H60H could be used as modulator for H60-specific CD8 T-cell responses. Altered peptide ligands for the OT-1 TCR epitope

have been intensively studied for their role in thymic selection [42]. A low-affinity peptide variants of Ova CD8 epitope, partial agonists or antagonist, induces positive selection of OT-1-beraing thymocytes. The affinity window for positive versus negative selection is narrow, and small changes can have big effects on the fates of immature thymocytes [43]. I do not know at present whether H60H would induce positive thymic selection of H60-specific CD8 T cells. Examination of the affinities of H60H-reactive and H60N-reactive T cells for both the H60N and H60H ligands in association with MHC I will provide a clue as to the role of H60H in thymic selection. H60 is an exceptionally dominant transplantation antigen. An H60-specific CD8 T-cell response can be detected even in the presence of a response against allo-MHC antigens [14] and is dominant over responses to other minor but dominant H antigens, such as H28, H4, H7, and HY [12]. The position of the H60H-specific CD8 T-cell response in the immune hierarchy relative to competing responses to MiHAs remains to be determined, as does the influence of H60H expression in the host on the dominance of the H60- specific CD8 T-cell response.

In summary, I have established a transgenic mouse line expressing a peptide mimic of the natural transplantation antigen H60. This system will be helpful in understanding the role of single amino acid variation in thymic selection of H60-reactive CD8 T cells and the mechanism of dominance of the H60-specific CD8 T cell response. In the future, this system might be used to develop a vaccination strategy to relieve GVHD symptoms and graft rejection through modulation of the H60-specific response.

CHAPTER 3

The role of myeloid-derived suppressor cells in the skin inflammation model

INTRODUCTION

BM-derived hematopoietic stem cells (HSCs) are recognized as self-renewing pluripotent cells capable of differentiating into a wide range of blood and immune cells. Recently, however, a role of HSCs in the repair of parenchymal tissue inflammation has received much attention. Following peripheral tissue injury, endogenous HSCs are activated and mobilized from the BM, migrate to the site of inflammation, and facilitate tissue repair and wound healing [44]. Similar effects were reported for exogenously implanted HSCs, which homed to the site of damage and contributed to tissue repair, suggesting their potential for use in regenerative medicine [44]. However, despite these well-accepted effects of stem cell-based therapies, the underlying cellular mechanism has not been elucidated completely. Migration to peripheral damaged sites and the pluripotent differentiation capacity of HSCs are the two major axes of their therapeutic potential. A growing number of molecular signals have been implicated in HSC migration. Multiple chemokines and proinflammatory cytokines (IL-1, IFN-α, IFN-β, TNF-α, and GM-CSF) produced at the site of inflammation were found to induce HSC-mobilization and

tissue recruitment [45]. Chemokine receptors, such as CXCR4 and CCR2, along with adhesion molecules expressed on HSCs mediate their homing to the BM, and are considered important regulators of tissue recruitment [46]. Other than these molecular studies, the detailed cellular dynamics of exogenous HSCs, including distribution/migration behavior in the recipients, have not been investigated extensively due to the lack of tools to properly analyze the rare infused cells in the recipients. In terms of differentiation, HSCs were shown to differentiate into activated $CD11b^{hi}F4/80^{lo}$ macrophages upon reaching the site of inflammation in a drug-induced liver injury model, indicating that the differentiation into these cells underlies a protective role for mobilized HSCs. Alternatively, in stroke, chronic heart disease, and hind limb ischemic models, HSCs were found to activate angiogenesis, which facilitated damage repair [47]. Otherwise, they differentiated into non-hematopoietic cells, contributing to the repair of skeletal and cardiac muscles, as well as skin injuries [48]. However, the underlying mechanism linking these various roles is unknown. Therefore, I conceived that longitudinal tracing of the differentiation of exogenous HSCs, in the context of *in vivo* dynamics including their

homing/distribution and proliferation, would be essential for understanding how administration of exogenous HSCs provides regenerative benefits in parenchymal tissue repair. To this end, I adopted various approaches to trace *in vivo* the fate of HSCs administrated exogenously. Bioluminescence imaging (BLI) analysis, which enables noninvasive *in vivo* cell monitoring [49], was used to track luciferase-transgenic stem cells *in vivo* for longitudinal detection of the distribution, proliferation, and persistence of stem cells in recipients with parenchymal tissue damage, and flow cytometric analysis was used to evaluate concurrent differentiation of stem cells on a single-cell basis. I exploited the advantage of the enhanced luciferase sensitivity displayed in a recently developed luciferase transgenic mouse, which was successfully used for tracing immune cells *in vivo* [50], and evaluated CD45.1 congenic marker expression in hematopoietic cells from $CD45.1^{+}$ mice using these mice as stem cell donors (sources) in BLI and flow cytometric analyses, respectively. As an animal model for tissue inflammation, I used a model of allergic contact dermatitis elicited experimentally by local skin treatment of the chemical 2,4-dinitrocholorobenzene (DNCB). The disease involves T cell activation, along with

infiltration of neutrophils and monocytic cells to the inflammatory lesion [51]. TNF-α, IL-1, and IFN-γ are produced at high levels, while IL-10 is detected at low levels, during the course of the disease [51]. This model allowed us to evaluate the anti-inflammatory effect of stem cell transplantation using the naked eye and to visualize migration of the luciferase-expressing stem cells to the inflamed skin more efficiently, as detection of luminescence signals is relatively straightforward if the signals emanate from locations in the vicinity of the body exterior, rather than the interior. Additionally, the well-established immunological pathogenesis of the disease facilitated investigation of the mechanism underlying the anti-inflammatory effect of the stem cells in an immunological context.

In this study, I performed longitudinal BLI and flow cytometric analyses of exogenously administered HSCs, using lineage-negative (Lin^-) cells in BM, which do not express lymphoid or myeloid lineage-markers. These approaches revealed that the therapeutic effects generated by transplanted Lin^- cells depend on their targeted migration to sites of inflammation and subsequent expansion. Intriguingly, I found that at the inflamed

site, these cells differentiated into myeloid-derived suppressor cells (MDSCs), which restrain the immune response in various settings, including cancer, inflammation and infection. Here, providing detailed information regarding the *in vivo* fate of exogenously administered HSCs, I demonstrate that expansion and concurrent differentiation into MDSCs *in situ* at the site of local inflammation are correlated with the therapeutic effect of HSC transplantation.

MATERIALS AND METHODS

1. Mice

C57BL/6 (B6) and B6.SJL-*Ptprc*^{a}*Pep3*^{b}/BoyJ (CD45.1^{+}) mice were purchased from the Jackson Laboratory (Bar Harbor, ME, USA). Transgenic luciferase mouse line (B6-Tg[CAG-effLuc]; B6-LucTg), which expresses modified firefly luciferase gene under control of actin promoter, has been described previously [50] and was maintained by crossing with B6 mice. All experiments were performed on mice between the ages of 8 and 12 weeks, and approved by the IACUC of Seoul National University. Mice were maintained under specific pathogen-free conditions at the Bio medical Center for Animal Resource Development of Seoul National University, College of Medicine, Korea.

2. Induction of skin dermatitis

Mice were sensitized on day 0 by epicutaneous application of 100 μL of 2% DNCB (2.4-dinitro-chlorobenzene; Sigma-Aldrich, St. Louis, MO, USA) in a 4:1 acetone:olive oil solution onto dry shaved back skin; a 4:1 combination of acetone and

olive oil was used as a vehicle control. After 5 days, the same amount of 2% DNCB solution was applied to both sides of the right ear of test group (n = 5), while the control group (n = 5) received the vehicle (acetone/olive oil). Clinical severity scores were graded on a scale of 0 to 4 (0, not present; 1, minimal; 2, slight; 3, moderate; 4, marked).

3. Histological analysis

Skin specimens were obtained on day 28 and fixed in 4% formaldehyde. Tissues were cut mid-sagittal, embedded in paraffin 24 h after fixation, and serially sectioned for histological analysis. Tissue sections were stained with hematoxylin and eosin (H&E) for analysis of general morphology.

4. BM cell isolation and Lin^- cell purification

Bone marrow cells were isolated from the femurs and tibiae of 8-week-old B6 mice. BM Lin^- cells were purified by magnetic cell-sorting (MACS) according to the manufacturer's instructions (Miltenyi Biotec, Auburn, CA, USA), using a BD Pharmingen Biotin Mouse Lineage Panel (San Jose, CA, USA).

MACS-purified Lin^- cells (5×10^6) were transplanted via tail vein injection into dermatitis mice.

5. In vivo imaging

In vivo bioluminescence imaging was performed using an IVIS 100 imaging system with a charge-coupled device (CCD) camera (Caliper Life Science, Waltham, Massachusetts, USA). Mice were placed on the imaging stage under anesthesia using 1.5% isoflurane gas in oxygen at a flow rate of 1.5 L/min, and were given an i.p. injection of the substrate, D-luciferin (150 mg/kg body weight; Molecular Probes, USA). Relative intensities of emitted light were presented as pseudocolor images ranging from red (most intense) to blue (least intense). Gray-scale photographs and the corresponding pseudocolor images were superimposed using the Living Image (ver. 2.12 Xenogen) and IGOR (WaveMetrics, Portland, OR, USA) image analysis software packages. Signals emitted by regions of interest (ROI) were measured and, data were expressed as photon fluxes (photon s/cm/sr), which refer to the photons emitted from a solid angle of a sphere. Data are presented as means ± SEM. Instrument background was subtracted

electronically, both from the images and from the measurements of photon flux.

6. Flow cytometric analysis

Single cell suspensions of BM and skin-infiltrating leukocytes were incubated at 4° C for 20 min in staining buffer (1X PBS with 0.1% bovine serum albumin and 0.1% sodium azide) containing the appropriate Ab mix. CD45.1-eFluor 450, Ly6G-FITC, CD11b-PE, F4/80-PE, CD115-APC, and Ly6C-APC Abs were obtained from eBioscience; CD11c-APC Ab and α-BrdU-FITC was purchased from BD Pharmingen. Data were collected using a FACSCalibur or LSRII-Green (both BD Pharmingen) and were analyzed using the FlowJo software.

7. Administration of drugs and antibodies

Mice were treated with FTY720 (2 μg/mL; Sigma-Aldrich) or 4-deoxypyrodixine hydrochloride (DOP; 30 μg/mL; Sigma-Aldrich) by direct addition to their drinking water. For the BrdU-incorporation assay, mice were injected intraperitoneally (i.p.) with 1 mg BrdU (Sigma-Aldrich) once daily for 4 days. For depletion of Gr-1-expressing cells, mice were injected i.p.

with 0.1 mg of either a rat anti-mouse Gr-1 Ab (BioXcell, Lebanon, NH, USA) or a control rat anti-mouse IgG Ab (BioXcell).

8. Quantitative RT PCR (qRT-PCR)

For RNA isolation, 2% DNCB solution was applied according to the same time schedule. RNA from the cells infiltrating inflamed skin or in BM, or whole tissues of the inflamed right ear were isolated using an RNeasy Micro RNA Kit (Qiagen, Valencia, CA, USA), and reverse-transcribed to generate cDNA using M-MLV reverse transcriptase (Takara Bio, Otsu, Shiga, Japan), 1× RT buffer, 0.25 mM dNTP, and 40 units RNase inhibitor (Koschem Co., Seoul, Korea). Quantitative PCR using the cDNA was performed as described by the manufacturer of SYBR premix ExTaq (Takara Bio) in 96-well plates on a thermal cycler (Light Cycler 96; Roche, Mannheim, Germany). Relative expression levels were calculated using the $2^{-\Delta\Delta Ct}$ method after normalization to beta-actin. The primer sequences are as follows: *Arg1*, forward 5’-ctccaagccaaagtccttagag-3, reverse 5’-aggagctgtcattagggacatc-3’; *Nos2*, forward 5-gttctcagcccaacaatacaaga-3’, reverse 5’-

aggagctgtcattagggacatc-3’; *Il10*, forward 5’-cagagaagcatggcccagaa-3’, reverse 5’-gtcaaattcattcatggccttgt-3’; *Tnfα*, forward 5’-ggaacacgtcgtgggataatg-3’, reverse 5’-ggcagactttggatgcttcttt-3’; *IL1β*, forward 5’-gcaactgttcctgaactcaac-3’, reverse 5’-atcttttggggtccgtcaact-3’; *Cd3*, forward 5’-atgcggtggaacactttctgg-3’, reverse 5’-gcacgtcaactctacactggt-3’; *Ly6g*, forward 5’-gtcccccaagccttgtgtg-3’, reverse 5’-aggtacttgtttagtgggaggg-3’; *Ly6c*, forward 5’-gcagtgctacgagtgctatgg-3’, reverse 5’-actgacgggtctttagtttcctt-3’; *Cd115*, forward 5’-tgtcatcgagcctagtgg-3’, reverse 5’-cgggagattcagggtccaag-3’; *b-actin,* forward 5′-ggctgtattcccctccatcg-3′; reverse, 5′-ccagttggtaacaatgccatg t-3′.

9. ELISA

Serum concentrations of TNF-α and IL-1β were measured by ELISA, according to the manufacturer’s protocol (BD Biosciences), and read at 450 nm using a microplate reader (BioTek, Winooski, VT, USA). All samples and standards were run in triplicate.

10. Statistical analysis

Statistical analysis was performed using GraphPad Prism (version 5, GraphPad Software, La Jolla, CA, USA). All error bars represent the standard error of the mean (SEM). P values were determined by Student's t-tests. (Unpaired two-tailed: $*P < 0.05$, $**P < 0.01$, $***P < 0.001$)

RESULTS

BM lineage−negative cells enhance skin regeneration in mice with contact hypersensitivity dermatitis

Contact dermatitis was induced as described previously [5]. Sensitization of the back skin of B6 mice with DNCB, followed by a secondary application to the ear 5 days later, induced severe inflammation at the site of exposure (Fig. 1A). Skin inflammation on the right ear peaked between 5 and 8 days after the secondary chemical application, and required more than 30 days before full recovery was evident (Fig. 1B−D; No transfer).

To examine the therapeutic effects of HSCs on skin regeneration in the DNCB−induced model of contact dermatitis, Lin^- cells were purified from BM and injected intravenously (i.v.) 1 day after the ear−challenge (Fig. 1A). As controls, both lineage−positive cells purified from BM (Lin^+) and PBS (no transfer) were administered in parallel. Regular observation and scoring of skin damage over the course of 1 month revealed that transplantation of Lin^- cells ameliorated skin inflammation, and improved the rate of tissue regeneration (Fig. 1, B−D). On day 28 post−transplantation of Lin^- cells, the damaged ear

showed reduced leukocyte infiltration, with reduced thickening of the epithelial layer, compared with the ears of control mice infused with Lin^+ cells or PBS (Fig. 1C), although full tissue regeneration had not yet occurred. In contrast, severe ear damage was prolonged in the case of mice transplanted with Lin^+ cells or PBS (Fig. 1B–D). Expression of IL-1β and TNF-α, inflammatory cytokines involved in DNCB-induced dermatitis [52], were significantly lower in both the inflamed ear skin and blood of Lin^- cell-transplanted mice, relative to Lin^+ and PBS controls (Fig. 1E and F). Together, these data indicated a marked therapeutic effect of transplanted Lin^- cells on skin inflammation in DNCB-induced dermatitis mice.

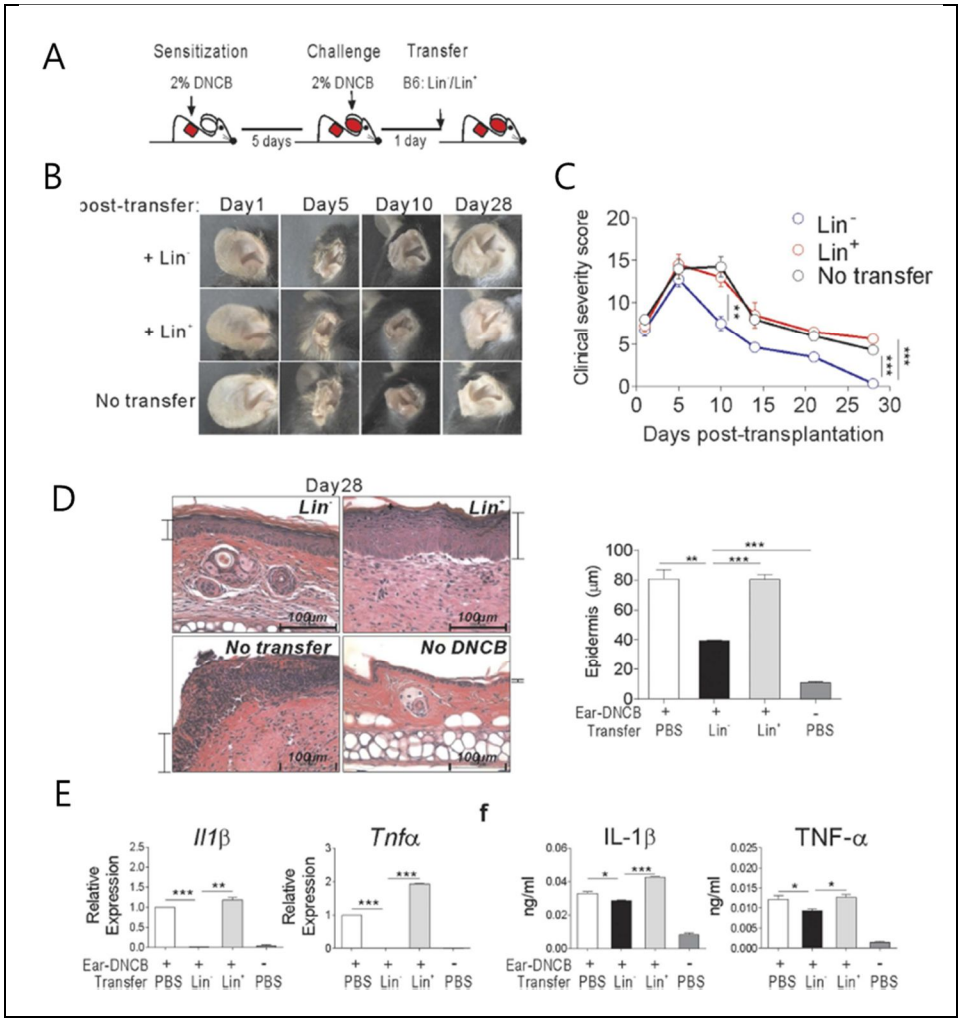

Figure 1. Transplantation of BM Lin⁻ cells enhances healing and skin regeneration in dermatitis mice.

(A) Schematic overview of DNCB treatment and Lin⁻ cell transplantation. Contact hypersensitivity dermatitis was induced in B6 mice by applying 2% DNCB solution to their shaved back, followed by a secondary challenge to the right ear 5 days later. One day after the secondary challenge, Lin⁻ or Lin⁺ cells (5 ×

10^6) isolated from the BM of normal B6 mice were injected i.v. into dermatitis mice. (B–C) The severity of ear skin inflammation after challenge with DNCB at several time points after transplantation (B), and the longitudinal clinical scores of these mice (C). Longitudinal photos of same mouse are presented in (B). Clinical severity scores in (C) were graded on a scale of 0 to 4, as described in Materials and Methods, periodically at 1 to 28 days after transplantation. (D) Histological examination of the inflamed ear skin of dermatitis mice receiving Lin^- or Lin^+ cell–transplantations, along with negative controls that received PBS (No transfer). Representative H&E stained images of mice harvested 28 days after transplantation are shown (Scale bar, 100 μ m); ear skin from control mice without DNCB treatment (no DNCB) was examined in parallel. Indications of epidermal layer are added to each image, with the depths of each experimental group are plotted. (E–F) Expression of IL-1β and TNF-α in the skin and blood of mice. (E) Relative expression of *Il-*β and *Tnf-*α were analyzed by qRT-PCR using RNA harvested from the skin tissue on day 14 post-transplantation. Delta-delta Ct values were normalized to those obtained from amplification of β -

actin and were expressed as fold changes compared to gene profiles of the DNCB with PBS-transfer sample. (F) Levels of IL-1β and TNF-α in the serum harvested from mice 14 days post-transplantation were measured by ELISA.

Longitudinal *in vivo* dynamics of transplanted Lin^- cells in the dermatitis mice.

To evaluate the mechanism by which exogenous Lin^- cells contribute to skin regeneration, I investigated the distribution and *in vivo* dynamics of Lin^- cells transplanted into DNCB-induced dermatitis mice via BLI analysis. First, Lin^- cells were isolated from the BM of luciferase transgenic mice (B6-LucTg mice), which express the firefly luciferase gene under control of the actin promoter [53]. These cells were then transplanted into tyrosinase mutant B6 mice (B6.Albino), which were used as a model for skin dermatitis because their white coat color facilitated detection, without absorption, of luminescence signals (Fig. 2A). B6.Albino mice receiving a primary DNCB-sensitization on the back only, followed by a secondary vehicle-only challenge were used as a control. Luminescence signals emanating from transplanted Lin^- cells were detected in the back and inflamed right ear within 12 h post-transplantation, with faint signals evident within 6 h in dorsal images (Fig. 2B). No luminescence was detected in the dorsal images of vehicle-control mice, indicating specific recruitment of Lin^- cells to the sites of inflammation.

Next, I tracked the signal intensity and location of transplanted cells in dermatitis mice over the course of 4 weeks. Luminescence signals from transplanted Lin^- cells were consistently strongest at the sites of inflammation (skin of back and right ear), with signal intensities increasing consistently over the first 14 days, implying a significant increase in the number of B6-LucTg Lin^- cells at these locations (Fig. 2C). Signal intensities emanating from the inflamed right ear peaked on day 14 post-transplantation, and waned significantly afterwards (Fig. 2D). In contrast, control mice exhibited only modest Lin^- cell signal intensities, in back skin (Fig. 2 C and D).

In the ventral images, Lin^- cell luminescence was detected at multiple BM sites in both dermatitis and vehicle-treated controls (Fig. 2E). This localization is thought to reflect their capacity as stem cells for selective homing to the BM, regardless of other conditions. However, when signal intensities in BM were plotted over time, it became apparent that increases in these signals were limited to mice with ear inflammation (Fig. 2F). A tibia BM site in the left foreleg was chosen as a region of interest (ROI) due to its physical distance from the abdomen where false positive luminescence signals were often generated

as a result of i.p. injection of the substrate luciferin. Longitudinal plotting of the single intensities of the BM at this site demonstrated that changes in the signal intensities of the BM were similar to those in inflamed ears in dorsal images.

A parallel experiment was also performed in which dermatitis or vehicle-treated control mice received Lin^+ cells isolated from B6-LucTg mice (Fig. 2 C-F). Lin^+ cells were detected in both inflamed ear and back skin, as well as in BM, albeit at levels significantly lower than those of Lin^- cells. Furthermore, these signals were only marginally increased by the presence of inflammation in the ears of dermatitis mice. Since Lin^- and Lin^+ cells purified from the BM of B6-LucTg mice express similar levels of the luciferase transgene, emitting similar levels of luminescence before transplantation (average of 0.38 and 0.49 $s/cm^2/sr$ per cell, respectively), any change in signal intensity was regarded as a change in the number of corresponding cells. Therefore, recruitment of Lin^- cells was specific to the sites of inflammation, with the expansion of these populations directly correlated with the degrees of inflammation. Additional expansion of Lin^- cells in the BM of dermatitis mice was also correlated with the extent of ear

inflammation in dermatitis mice.

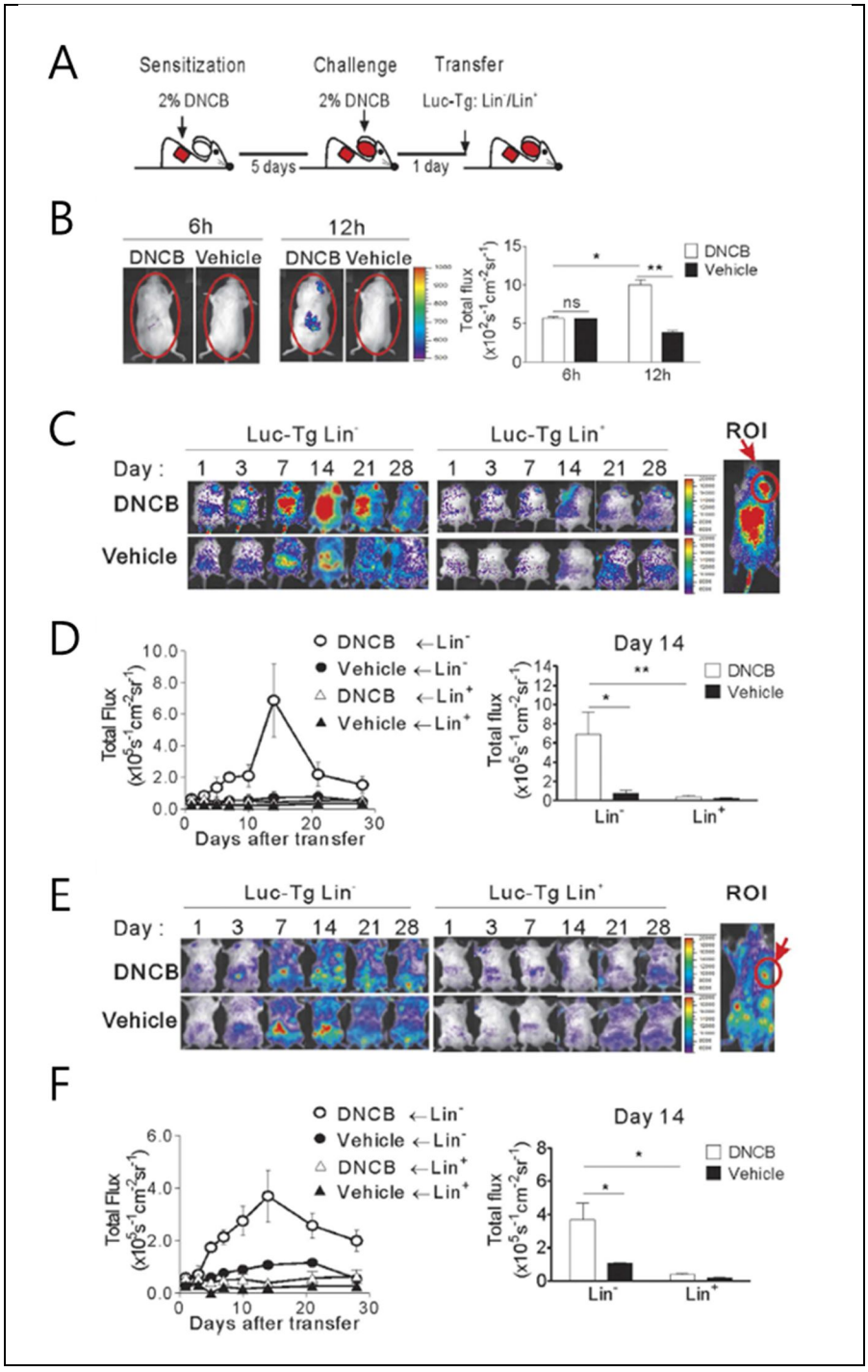
A
Sensitization
2% DNCB
Challenge
2% DNCB
Transfer
Luc-Tg: Lin-/Lin+
5 days
1 day
B
6h
12h
DNCB Vehicle
DNCB Vehicle
Total flux
(x10²s⁻¹cm⁻²sr⁻¹)
ns
*
**
DNCB
Vehicle
6h
12h
C
Luc-Tg Lin-
Luc-Tg Lin+
ROI
Day :
1 3 7 14 21 28
DNCB
Vehicle
D
DNCB ←Lin-
Vehicle ←Lin-
DNCB ←Lin+
Vehicle ←Lin+
Total Flux
(x10⁵s⁻¹cm⁻²sr⁻¹)
Days after transfer
Day 14
Total flux
(x10⁵s⁻¹cm⁻²sr⁻¹)
Lin-
Lin+
E
Luc-Tg Lin-
Luc-Tg Lin+
ROI
Day :
1 3 7 14 21 28
DNCB
Vehicle
F
DNCB ←Lin-
Vehicle ←Lin-
DNCB ←Lin+
Vehicle ←Lin+
Total Flux
(x10⁵s⁻¹cm⁻²sr⁻¹)
Days after transfer
Day 14
Total flux
(x10⁵s⁻¹cm⁻²sr⁻¹)
Lin-
Lin+

Figure 2. In vivo dynamics of transplanted Lin^- cells in dermatitis mice.

(A) Schematic overview of DNCB-treatment and Lin^- or Lin^+cell transplantation. Lin^- and Lin^+ cells were isolated from Luc-Tg mice. (B) Bioluminescence images were taken 6 and 12 h post-transplantation of Luc-Tg cells (5×10^6). Dorsal images are shown. Total photon counts were generated using the entire dorsal area of the mouse as the region of interest (ROI). (C-D) Longitudinal dorsal bioluminescence images. (C) Representative dorsal images of dermatitis or control mice transplanted with Luc-Tg Lin^- or Lin^+ cells (5×10^5) were taken on days 1, 3, 7, 14, 21, and 28 post-transplantation. The inflamed right ear was designated as the ROI. (D) Photon flux values emanating from the right ear of the mice were plotted longitudinally. Peak signal values were compared between experimental groups on day 14 post-transplantation. (E-F) Longitudinal ventral bioluminescence images. Ventral images were processed as above (C-D) after designation of the upper tibia as the ROI.

Homing and expansion of transplanted Lin^- cells in the BM and inflamed skin of dermatitis mice.

The similar expansion kinetics of Lin^- progenies in the inflamed skin and BM suggested that Lin^- cells home to the skin and BM almost immediately after transplantation, although the signals from BM were rarely detected in the ventral BLI data at early time points (data not shown). To examine this on a single-cell basis, I performed flow cytometric analysis of cells infiltrating the inflamed skin and BM of $CD45.2^+$ B6 dermatitis mice following transplantation of 5-chloromethylfluorescein diacetate (CMFDA)-labeled $CD45.1^+Lin^-$ cells. CMFDA-positive ($CMFDA^+$) cells were detected among the cells infiltrating the inflamed skin and in the BM of the upper tibia at 6 and 12 h post-transplantation (Fig. 3A, B). The $CMFDA^+$ cells in the inflamed skin were of lineage marker-negative status at 6 h (Fig. 3C). Taken together, these data indicate early or immediate homing of Lin^- cells, following upon transplantation into inflamed sites as well as the BM. The absolute numbers of transplanted ($CMFDA^+$ or $CD45.1^+$) cells in the inflamed skin of dermatitis mice increased between 6 and 12 h (Fig. 3A), up to an average of 3.2×10^4 cells (4.4% of

leukocytes in the inflamed skin) on day 14 post-transplantation (Fig. 3D). However, these absolute numbers in the inflamed skin were lower than those in the BM of the dermatitis mice even at 6 h (Fig. 3B), signifying that homing to the BM was a major event following transplantation, even with a subpopulation of these cells similar between the dermatitis mice and vehicle-control mice at 6 h post-transplantation, but eventually increased significantly (up to 2.8% of BM cells) in the dermatitis mice on day 14 post-transplantation (Fig. 3E). This transient stagnation of Lin^- cells in BM of the dermatitis recipients may be due to the presence of continued recruitment of Lin^- cells to inflamed sites by the 12 hr time point, while such recruitment rarely occurring in the control mice. Such substantial increase in the $CD45.1^+Lin^-$ progenies in the inflamed skin and BM observed only in dermatitis mice, compared with control mice, is consistent with the BLI data (Fig. 2). $CD45.1^+Lin^+$ cells were also recruited to the site of inflammation and to the BM of dermatitis mice (Fig. 3C); however, their proportions and absolute numbers were significantly lower in both locations than those of $CD45.1^+Lin^-$ progenies on day 14 (Fig. 3D,E).

Taken altogether, these data demonstrate considerable early homing of transplanted Lin^- cells to inflamed skin as well as to the BM, and subsequent expansion of the progenies at both sites in the dermatitis mice, confirming the BLI studies.

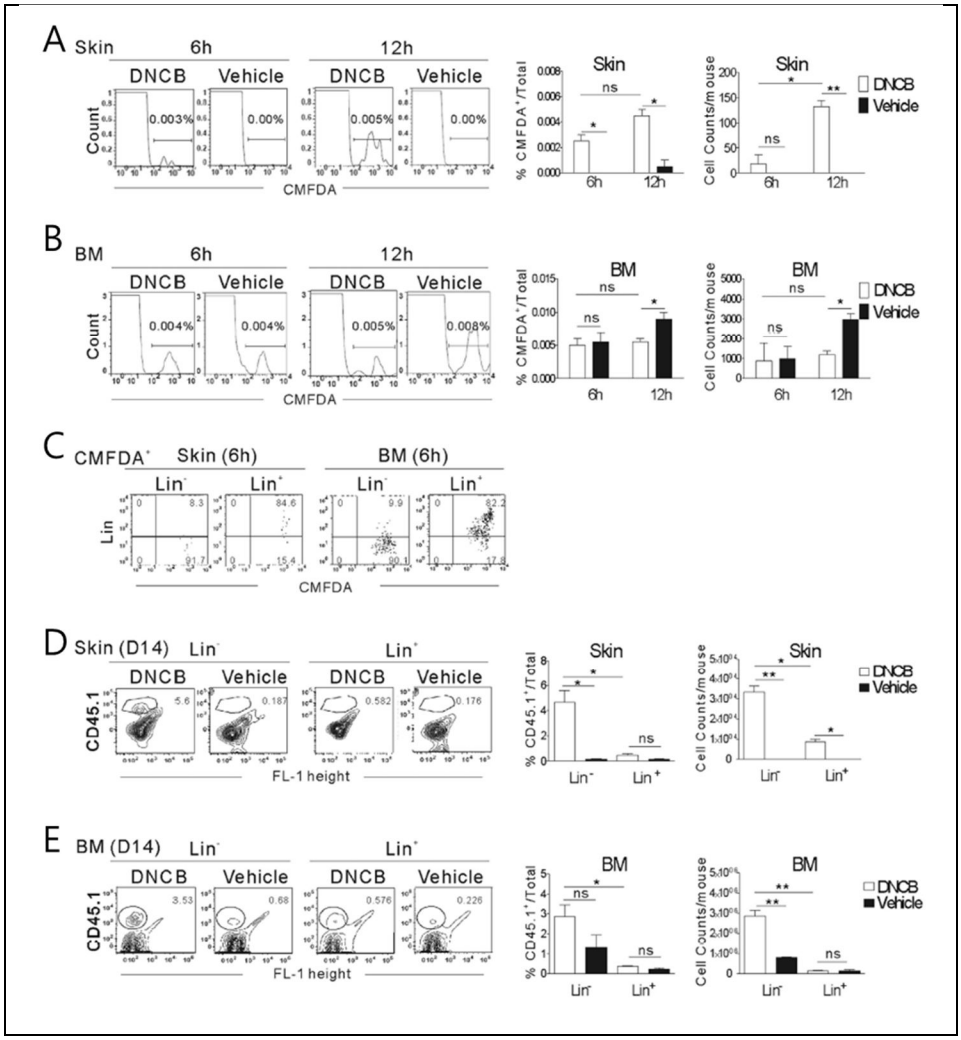

Figure 3. Early homing and expansion of Lin^- cells at the site of inflammation and BM.

(A–C) Flow cytometric analysis of $CMFDA^+$ cells in inflamed skin and BM at 6 and 12 h after transplantation of $CMFDA^+CD45.1^+Lin^-$ cells. Dermatitis or vehicle-control $CD45.2^+$ B6 mice were transplanted with CMFDA-labeled Lin^- cells or Lin^+ cells (1×10^6), and analyzed for the presence of

$CMFDA^+$ cells in the inflamed skin and BM at 6 and 12 h after the transplantation by flow cytometry; representative flow cytometric data are shown. The percentage of $CMFDA^+$ cells in the leukocytes present in skin (A) or BM cells (B), and the numbers of $CMFDA^+$ cells in the skin and BM per mouse are shown. (C) Flow cytometric analysis of lineage marker expression in $CMFDA^+$ cells in inflamed skin and BM at 6 h post-transplantation of CMFDA-labelled $CD45.1^+Lin^-$ or Lin^+ cells. Representative data are shown. (D-E) Flow cytometric analysis of $CD45.1^+$ cells in inflamed skin (D) and BM (E) 14 days post-transplantation of $CD45.1^+Lin^-$ or Lin^+ cells; representative data are shown. Data were processed as described in (A-B).

In situ proliferation of progenies of transplanted Lin^- cells in the inflamed skin.

I wondered whether the signal increases observed at the site of inflammation 14 days post-transplantation were the result of in situ proliferation of Luc-Tg Lin^- progenies already present in the inflamed skin, or constant influx of cells originally homing to the BM. To resolve this, I treated dermatitis mice with the cell egress blockers FTY720 or 4-deoxypyridoxine (DOP), which retain cells in BM for 24 h [54], continuously from one day after transplantation of Luc-Tg Lin^- cells, and monitored the increase in the luminescence signal in the inflamed ear (Fig. 4A). Continued exposure to cell-egress blockers over 3 days failed to inhibit signal increases in the inflamed skin (Fig. 4B), with an average 1.7- or 1.5-fold increase in signal intensities detected in the inflamed ear skin during the drug treatment period (day 3/day 1 post-FTY720 or DOP treatment, respectively). This indicated that in situ expansion of Lin^- progenies at the site of inflammation contributed to the signal increase in the absence of a cellular influx from the BM. However, these fold-change values were slightly lower, albeit not significantly so, compared to the values (2.0-fold on

average) in the DW-treated group. Therefore, it is possible that cellular influx from the BM also contributes to the increase in Lin^- progenies in the inflamed skin in the absence of such a BM-egress blockade. Flow cytometric analyses of mice treated with the cell egress blocker FTY-720 revealed a marked increase in the proportion of $CD45.1^+$ cells in the inflamed skin of dermatitis mice, indicative of in situ expansion of these cells in the absence of cellular egress from BM. However, their absolute number in the inflamed skin was lower in the presence of cell egress blockers relative to DW-fed controls (Fig. 4C). Therefore, in addition to their proliferation at inflamed sites, influx of cells from the BM also accounted for the increase in the $CD45.1^+$ Lin^- progenies in the inflamed skin. FTY720 treatment enhanced both the percentages and numbers of $CD45.1^+$ cells in the BM, verifying the blockade of cell egress from BM during drug treatment. The presence of in situ proliferation of Lin^- progenies was further confirmed by the presence of BrdU-positive cells among the $CD45.1^+$ cells in inflamed skin, following BrdU administration after initiation of FTY-720 treatment (Fig. 4D).

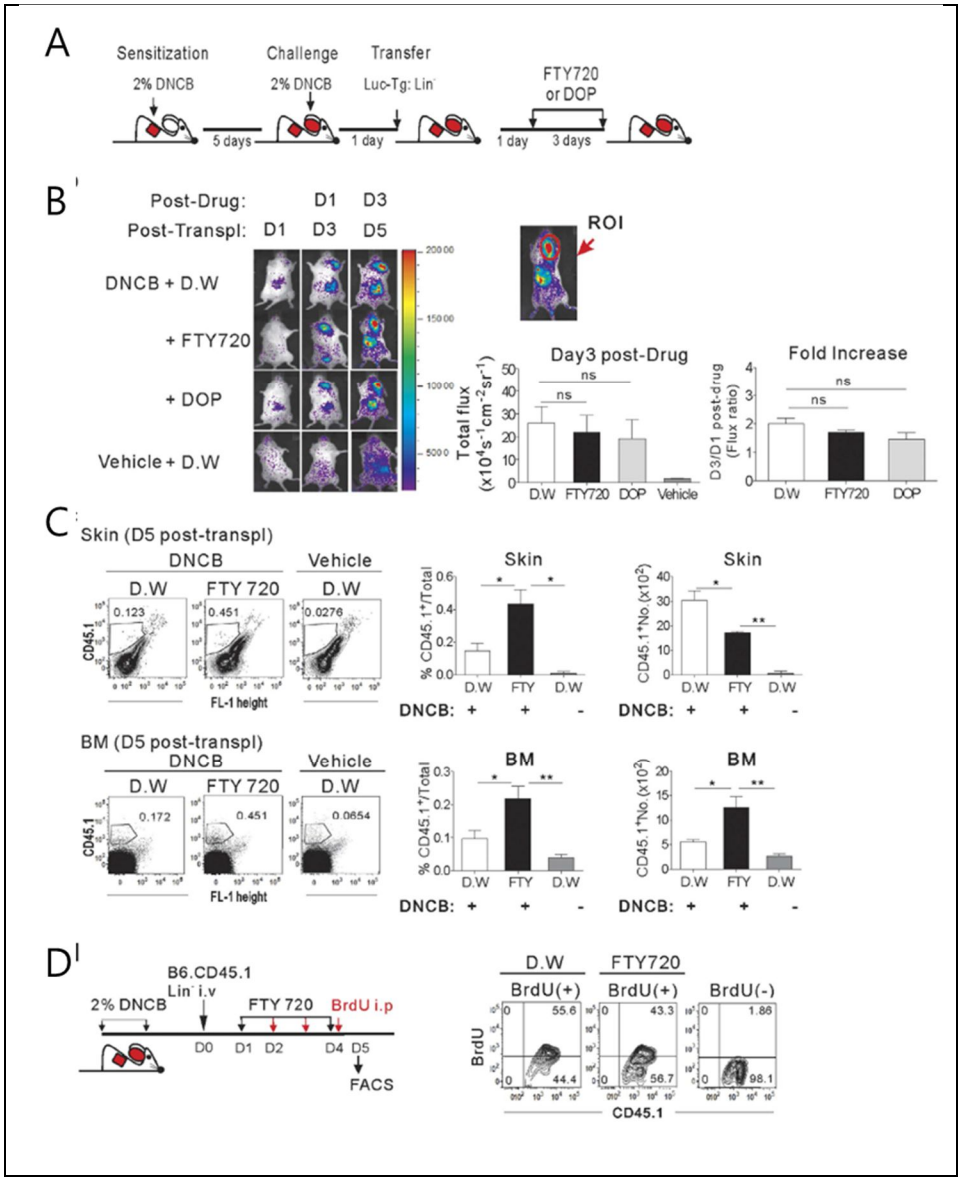

Figure 4. In situ proliferation of Lin⁻ cells at the site of inflammation.

(A) Schematic overview of DNCB treatment, Lin⁻ cell transplantation, and BM egress inhibition. FTY-720 or DOP was added to the drinking water for 3 days, beginning 1 day

after transplantation of Lin^- cells. (B) Dorsal bioluminescence images of transplanted (5×10^5 of Luc-Tg Lin^- cells) and drug-treated mice. Total photon flux values from the right ear were measured, and fold increases between days 1 and 3 post-drug treatment are shown. (C) Flow cytometric analyses of $CD45.1^+Lin^-$ cells in the skin and BM of the transplanted (1×10^6 of Lin^- cells from $CD45.1^+$ mice) and drug-treated dermatitis mice on day 5 post-transplantation; representative data are shown. The percentage of $CD45.1^+$ cells in the leukocytes present in skin or BM cells and the numbers of $CD45.1^+$ cells in the skin and BM per mouse are plotted. (D) DNCB-treated, $CD45.1^+Lin^-$ cell-transplanted, and FTY-720-treated mice were injected with 1 mg of BrdU daily for 3 days. FTY-720 was added to drinking water continuously until day 4 starting from day 1 post-transplantation. Leukocytes were isolated from the skin and stained with anti-CD45.1-APC and anti-BrdU-FITC Abs. Representative flow cytometric data shown are gated for $CD45.1^+$ cells.

Transplanted Lin^- cells differentiate into myeloid and granulocytic cells.

Having established the source of cells expanded at the site of inflammation, I next investigated differentiation of Lin^- progenies at the site of inflammation, as these processes were presumed to play a role in their therapeutic effects. To determine the lineage of the differentiating cells, I selectively depleted each cell lineage by treating the recipients with Abs against lineage markers (Gr-1, CD4, CD8, or B220) prior to and 3 days after transplantation of Luc-Tg Lin^- cells (Fig. 5A). Then, differentiation into a specific lineage was determined by specific signal abrogation in the recipients with the corresponding depletion treatment in BLI analyses. Treatment with a Gr-1-depleting Abs abrogated the luminescence signals at the site of inflammation when the recipients of Luc-Tg Lin^- cells were analyzed on day 7, but not on days 1 or 3 post-transplantation (Fig. 5B), as did clodronate-treatment which depletes macrophage/monocytes *(data now shown)*. This indicated depletion of Gr-1-expressing cells originated from transplanted Luc-Tg Lin^- cells in the inflamed skin on day 7. Prior flow cytometric analysis had verified depletion of $Gr\text{-}1^{hi}$

granulocytes in the inflamed skin of dermatitis mice with one time treatment of anti-Gr-1 Ab *(data not shown).* Other treatments including those targeting CD8, CD4, and B220 had no effect on signal detection (data not shown). These results indicated that, despite their multi-lineage potency, Lin^- cells preferentially differentiated into myeloid and granulocytic lineage cells within the first 7 days, in consistent with the promoted myeloid/granulocytic differentiation in the presence of inflammation, relative to steady-state hematopoiesis [52].

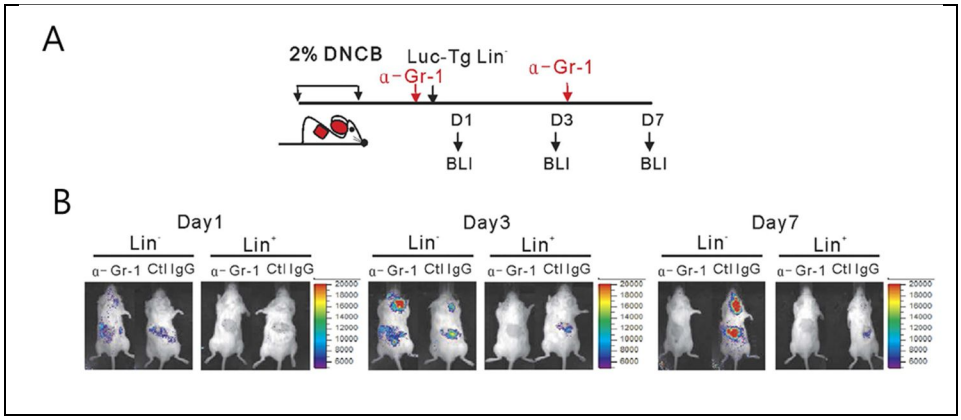

Figure 5. Differentiation of Lin− cells into myeloid and granulocytic cells at the site of inflammation.

(A) Schematic overview of treatment with anti−Gr−1 depleting Abs and transplantation of Lin^- or Lin^+ cells (5×10^5). Dermatitis mice were injected i.p. with an anti−Gr−1 Ab prior to and 3 days after transplantation with Luc−Tg Lin^-cells; rat−IgG was treated as a control. (B) BLI images were collected on days 1, 3, and 7 post−transplantation.

Myeloid/granulocytic differentiation of transplanted Lin^- cells occurs similarly in inflamed skin and BM.

To better characterize the myeloid lineage of Lin^- progenies, I used flow cytometry to examine $CD45.1^+$ cells in the inflamed skin on days 5 and 7 post-transplantation of $CD45.1^+Lin^-$ cells when the ear inflammation was severe, and on day 14 when the skin inflammation subsided significantly (Fig. 1), supposing that healing effects of Lin^- cell transplantation would be exerted before inflammation begins to subside. Lin^- cells isolated from $CD45.1^+$ donor mice were negative for CD11b and Gr-1 (Ly6G and Ly6C; Fig. 6A), as well as B220, CD3, Ter119 and CD11c expression *(data not shown)*. However, when analyzed on day 5 post-transplantation, all of the $CD45.1^+$ cells of donor origin were $CD11b^+$ (Fig. 6B), consistent with a myeloid cell lineage. A large majority ($\geq$ 80%) of $CD11b^+$ cells exhibited a $Ly6G^{int}Ly6C^+$ phenotype on days 5 and 7 post-transplantation. However, on day 14, the proportions of $Ly6G^{int}Ly6C^+$ cells were reduced dramatically (33.6% on average), although their absolute numbers were not changed significantly, compared to those on day 7. Instead, $Ly6G^{hi}Ly6C^{low}F4/80^-$ neutrophils were detected at larger proportions (43%), with their numbers being

significantly increased, along with $Ly6G^{low}Ly6C^{low}$ (9.6%) and $Ly6G^{-}Ly6C^{low}$ (7.4%) cells, which were composed of $F4/80^{+}$macrophages and $CD11c^{+}$ dendritic cells. $CD11b^{+}Ly6G^{int}Ly6C^{+}$ was the phenotype of the BrdU-incorporating cells undergoing in situ proliferation at the inflamed skin site during the period of FTY-720 BM-egress blocker treatment (Fig. 6C), suggesting that proliferating cells in situ would differentiate into $CD11b^{+}Ly6G^{int}Ly6C^{+}$ cells in the inflamed skin. A majority of the $Ly6G^{int}Ly6C^{+}$ cells on days 7 and 14 were positive for F4/80, but the surface F4/80 levels were higher on the day 14-cells, indicating that these cells are more matured status compared to day 7-cells. Taken together, these data show the predominance of the $Ly6G^{int}Ly6C^{+}$ cells with in situ proliferative potential over the first 7 days and the later appearance of other myeloid cells in the inflamed skin on day 14, and suggest that the $CD11b^{+}Ly6G^{int}Ly6C^{+}$ cells might be the precursors of the late appearing matured myeloid cells. Interestingly, compositions of $CD45.1^{+}Lin^{-}$ cells in the BM at the same time points post-transplantation were quite similar to those in inflamed skin, with the $Ly6G^{int}Ly6C^{+}F4/80^{+}$ cells representing the major population among the $CD45.1^{+}$ cells in

BM, at days 5 and 7 post-transplantation (Fig. 6D). In contrast to the dynamic changes in myeloid populations derived from Lin^-cells over time, progenies of transplanted Lin^+ cells comprised $Ly6G^{hi}Ly6C^{low}F4/80^-$neutrophils (≥ 60%), along with smaller proportions of $Ly6G^{int}Ly6C^+F4/80^+$ (24.5% on average) and $Ly6G^-/^{low}Ly6C^{low}$ cells (≤ 10%) in the inflamed skin (Fig. 6A). Unlike Lin^- cells, the relative proportions of these cell populations remained stable throughout the analysis period, indicating a clear difference between Lin^- and Lin^+ cells. These data led to us conclude that transplanted Lin^- cells preferentially differentiated into cells of myeloid and granulocytic lineage in the inflamed skin as well as in the BM of dermatitis mice with similar kinetics. Moreover these results demonstrated that transplanted Lin^- cells differentiated mostly into $CD11b^+Ly6G^{int}Ly6C^+$ cells with proliferative potential on days 5-7 post-transplantation, when the inflammation was most severe.

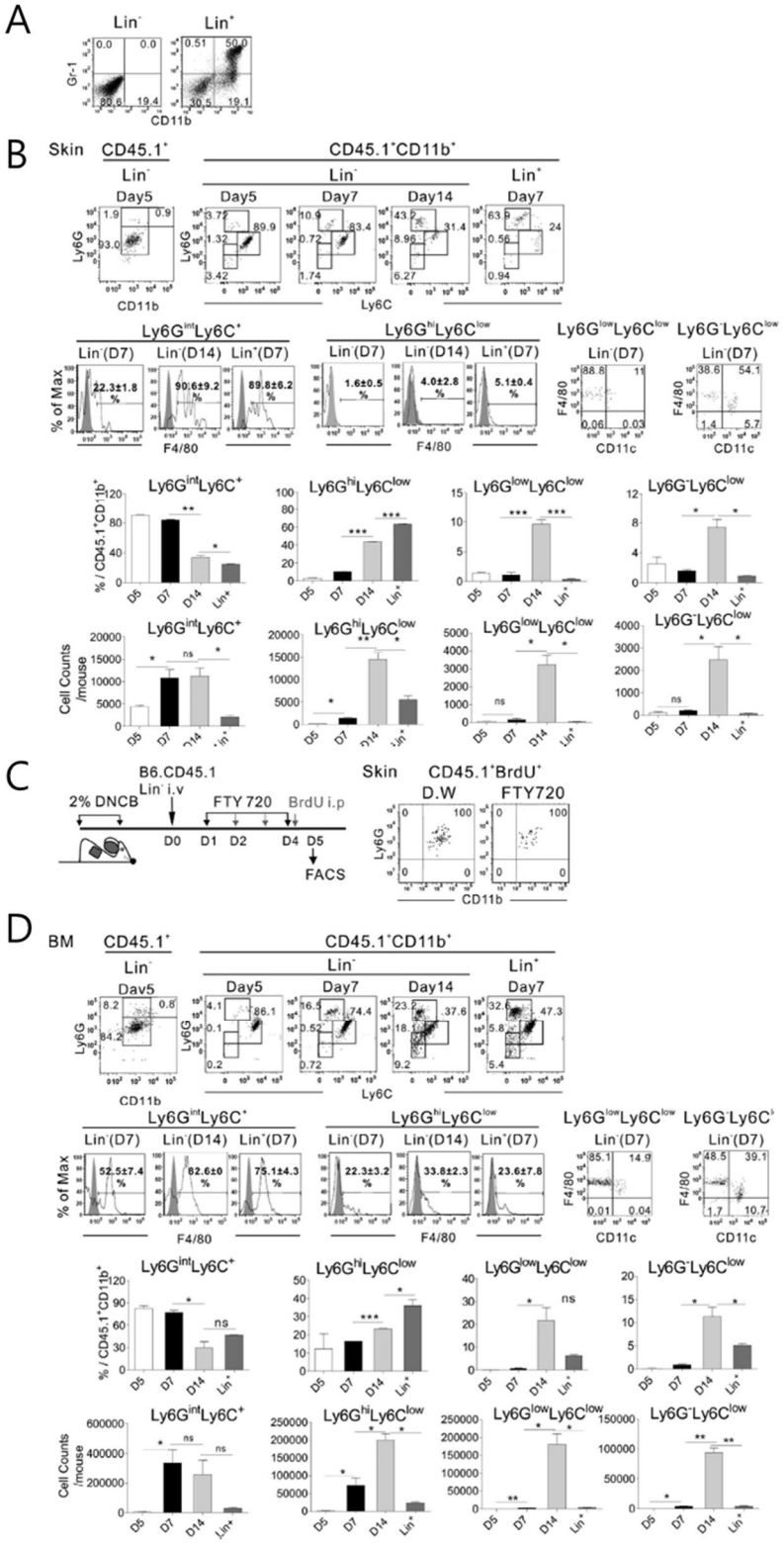
A
Lin-
Lin+
Gr-1
CD11b
B
Skin
CD45.1+
CD45.1+CD11b+
Day5
Day7
Day14
Ly6G
Ly6C
CD11b
Ly6GintLy6C+
Ly6GhiLy6Clow
Ly6GlowLy6Clow
Ly6G-Ly6Clow
Lin-(D7)
Lin-(D14)
Lin+(D7)
% of Max
F4/80
CD11c
% / CD45.1+CD11b+
Cell Counts /mouse
C
B6.CD45.1
Lin- i.v
2% DNCB
FTY 720
BrdU i.p
D0
D1
D2
D4
D5
FACS
Skin
CD45.1+BrdU+
D.W
FTY720
D
BM

Figure 6. Differentiation of $CD45.1^{+}Lin^{-}$ cells into myeloid and granulocytic lineages in the inflamed skin and BM of the dermatitis mice.

(A) Flow cytometric analysis of Lin^{-} or Lin^{+} cells purified for transplantation. (B) Flow cytometric analysis of $CD45.1^{+}$ cells in the inflamed skin of dermatitis mice transplanted with $CD45.1^{+}Lin^{-}$ or Lin^{+} cells (1×10^{6}) at various time points after transplantation. $CD45.1^{+}$ cells isolated from the skin were analyzed for expression of CD11b, Ly6G, Ly6C, F4/80, and CD11c on the designated days post-transplantation. Representative data gated for $CD45.1^{+}$ cells are shown. Percentage values of each population within the $CD45.1^{+}CD11b^{+}$ cells and absolute cell numbers are shown. (C) DNCB-treated, $CD45.1^{+}Lin^{-}$ cell-transplanted, and FTY-720-treated mice were injected with 1 mg BrdU daily for 3 days. FTY-720 was added to drinking water continuously until day 4 starting from day 1 post-transplantation. Leukocytes were isolated from the skin and stained with anti CD45.1-eFluor 450, anti- CD11b APC, anti--Ly6G PE and anti-BrdU-FITC Abs. Representative data gated for $CD45.1^{+}BrdU^{+}$ cells are shown (D) Flow cytometric analysis of $CD45.1^{+}$ cells

in the BM. Data were analyzed as described above; representative data gated for $CD45.1^+$ cells are shown.

Enhanced differentiation of Lin^- cells into $CD11b^+Ly6G^{int}Ly6C^+CD115^+$ MDSCs in the inflamed skin.

The $CD11b^+Ly6G^{int}Ly6C^+$ phenotype with proliferative potential is consistent with their classification as MDSCs, which have been well characterized to have an immunosuppressive function in tumor environments [53]. Mouse MDSCs are known to express CD115 [55]. Thus, I examined the expression of CD115 by the $Ly6G^{int}Ly6C^+$ cells of transplanted $CD45.1^+Lin^-$ cell origin in the inflamed skin and BM on day 7, after which disease scores decrease (Fig. 1C), implying a high probability that Lin^- progenies are exerting suppressive function about the time point. The proportion of $CD115^+$ cells in the predominant $Ly6G^{int}Ly6C^+$ cell population was significantly elevated (62.4% on average) in the inflamed skin, with little decrease in the proportion of $CD115^+$ cells among the minor $Ly6G^{hi}Ly6C^+$ cell population (24.45%; Fig. 7A). Unexpectedly, however, proportions of $CD115^+$ cells were significantly lower (27% on average) among the $Ly6G^{int}Ly6C^+$ cells in the BM. These results show that, despite the similarity in the overall phenotypes of the $Ly6G^{int}Ly6C^+$ cells between the inflamed skin and BM, differentiation into $CD115^+$ cells was preferential in

the inflamed skin. As an additional control, Lin^+ cells in inflamed skin comprised low proportions of $CD115^+$ cells (19.3% on average). Next, I evaluated the suppressive functions of the $CD45.1^+$ cells present in the inflamed skin and BM on day 7 post-transplantation of $CD45.1^+Lin^-$ cells. In immune-suppression assays, co-culture with skin-derived $CD45.1^+$ cells suppressed proliferation of CD3/CD28-stimulated T cells, reducing their CFSE-dilution (33% on average). However, $CD45.1^+$ cells isolated from BM allowed more than 86% of the co-cultured T cells to proliferate (Fig. 7B), to the same extent as did Lin^+ cells isolated from inflamed skin *(data not shown).* Moreover, the suppressive activity of skin-derived $CD45.1^+$ cells was relieved when an iNOS-inhibiting agent, NG-methyl-L-arginine acetate (L-NMMA), was added to co-cultures of activated T cells and skin-derived $CD45.1^+$ cells (Fig. 7C). These results demonstrated that the $Ly6G^{int}Ly6C^+$ cells present in the inflamed skin would become MDSCs with an iNOS-dependent immune suppressive function [53]. When the expression levels of anti- and pro-inflammatory genes were examined, it was revealed that both iNOS and Arginase-1, representative genes related to MDSC function [53], as well as

the anti-inflammatory cytokine Il10, were expressed in skin-derived CD45.1$^+$ cells at significantly higher levels, compared with their BM counterparts (Fig. 7D). Relatively higher expression of Arginase-1 and iNOS in the skin-derived CD45.1$^+$ cells was confirmed by flow cytometric analysis (Fig. 7E). Also, higher expression of Cd115 in the skin-derived CD45.1$^+$ than the other cells (BM-counterparts and Lin$^+$ cells) was verified. In the case of pro-inflammatory cytokines, Tnfα expression in the CD45.1$^+$Lin$^-$ progenies in inflamed skin was significantly lower than that in CD45.1$^+$ Lin$^+$ cells (Fig. 7D), while their Il1β expression was not significantly different from the Il1β expression in transplanted Lin$^+$ cells. These results indicated the biased differentiation of transplanted Lin$^-$ cells into MDSCs with immune-suppressive function in the inflamed skin. Although CD3$^+$ T cells were hardly detectable in flow cytometric analyses of skin-infiltrating cells on day 7 (*data now shown)*, gene expression analyses of the inflamed skin tissues demonstrated that *Cd3* transcript levels in the inflamed skin were significantly lower in the mice receiving Lin$^-$ cells than in those receiving Lin$^+$ cells or PBS, indicating a relatively lower overall abundance of CD3$^+$ T cells in the inflamed skin of

the Lin^- cell-recipients. In support of this, flow cytometric analyses after staining the cells with anti-CD4 and -CD8 Abs instead of anti-CD3 Ab demonstrated that proportions of $CD4^+/CD8^+$ cells in the skin-infiltrating cells were smaller in the Lin^- cell recipients than in the Lin+ cell or PBS recipients (Fig. 7G). This indicates the possibility of CD3-down-modulation by T cells activated in the inflamed skin. Variable levels of Ly6g, Ly6c, and Cd115 were detected in the inflamed skin of each group, reflecting the relatively high frequencies of $Ly6G^{int}Ly6C^+$ $CD115^+$ cells in the skin of Lin^- cell-recipients and of $Ly6G^{hi}Ly6C^{low}$ neutrophils in the skin of the Lin^+ cell-recipients. Together, these data demonstrate that differentiation of transplanted Lin^- cells in the inflamed skin was biased toward $CD11b^+Ly6G^{int}Ly6C^+CD115^+$ MDSCs with immunosuppressive functions in the inflamed skin, compared with the BM. Such skewed differentiation may be the cellular mechanism which promotes skin healing that follows Lin^- cell transplantation noted in recipient mice.

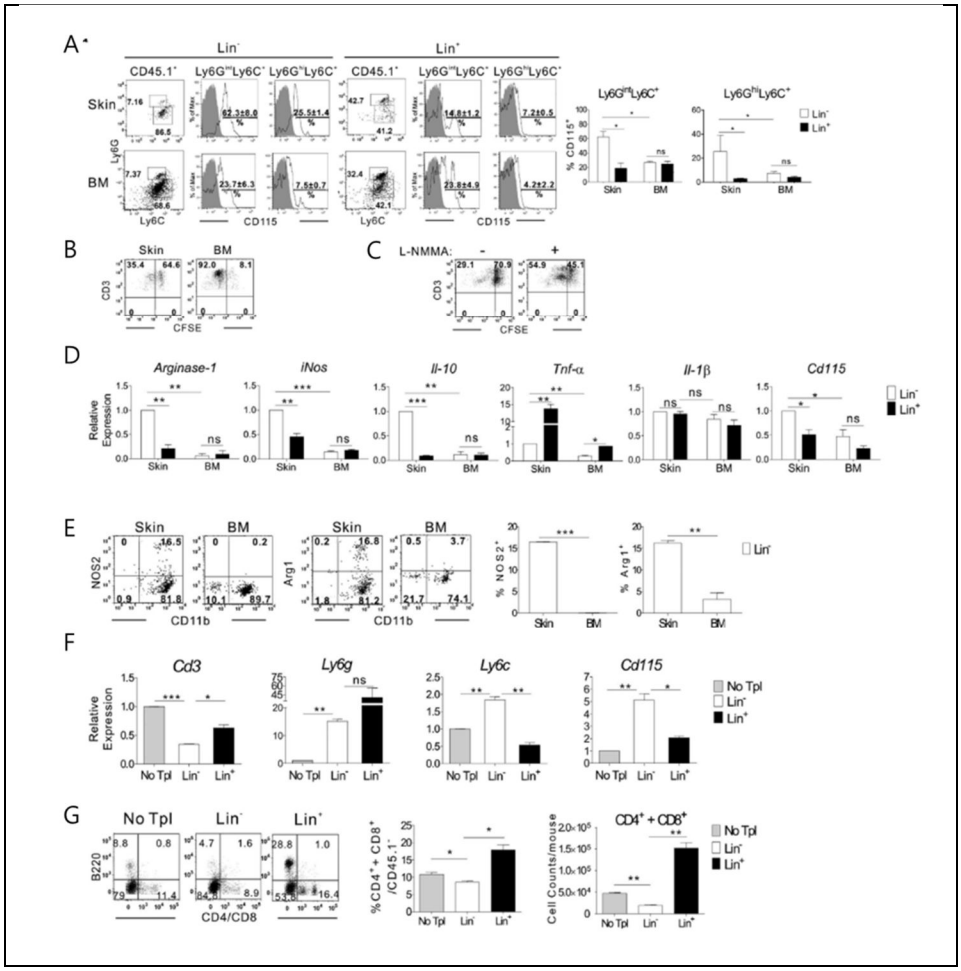

Figure 7. Differentiation of $CD45.1^{+}Lin^{-}$ cells into $CD115^{+}$ MDSCs in inflamed skin.

(A) Flow cytometric analysis of $CD45.1^{+}$ cells in the inflamed skin and BM of recipients of $CD45.1^{+}Lin^{-}$ or Lin^{+} cells on day 7 post-transplantation. $CD45.1^{+}$ cells were analyzed by flow cytometry and representative data are shown. Percentage values of $CD115^{+}$ cells within the $CD11b^{+}Ly6G^{int}Ly6C^{+}$ and $CD11b^{+}Ly6G^{hi}Ly6C^{+}$ cell populations are plotted. (B-C)

Immune suppression assays of $CD45.1^+$ cells isolated from the inflamed skin or BM (B), or those from skin in the presence (+) or absence (−) of L−NMMA (1mM). CFSE dilution by CFSE−labeled $CD3^+$ T cells was analyzed via flow cytometry after stimulation in the presence sorted $CD45.1^+$ cells. (D) QRT−PCR analysis of $CD45.1^+$ cells isolated from the skin and BM. Relative levels of transcripts expressed by $CD45.1^+$ cells in the BM and skin of mice transplanted with Lin^- cells and Lin^+ cells were compared. Delta−delta Ct values were normalized to those obtained from amplification of *β -actin* and were expressed as fold changes compared with gene profiles of Lin^- cells in inflamed skin. (E) Flow cytometric analysis for expression of CD11b and NOS2 by $CD45.1^+$ cells in the inflamed skin and BM of recipients of $CD45.1^+Lin^-$ cells on day 7. Representative flow cytometric data are shown, and the percentage values of $NOS2^+$ or arginase−1^+ cells within the $CD45.1^+$ cell populations are plotted. (F) QRT−PCR analysis using RNA extracted from the inflamed skin of Lin^- or Lin^+ cell recipients, along with negative control mice that received PBS (no Tpl; no transplantation). Relative transcript levels are shown. Normalized values are expressed as fold changes

compared with gene profiles of the no transplantation sample. (G) Flow cytometric analysis of skin-infiltrating cells after staining with anti-CD4-PE, anti-CD8-PE, anti-B220-APC, anti-CD45.1-eFlour 450 antibodies on day 7 post-transplantation. Representative flow cytometric data are shown after $CD45.1^-$ cell gating.

DISCUSSION

In this study, via a longitudinal in vivo analysis of transplanted Lin^- cells in a murine model of contact dermatitis, I demonstrated that transplanted stem cells were recruited to the inflamed skin and underwent expansion and differentiation into $CD11b^+Ly6G^{int}Ly6C^+$ immune-suppressive cells therein. HSCs are recruited to sites of tissue damage in several injury and disease models [44]. Consistently, I showed recruitment of exogenous Lin^- cells to inflamed skin upon transplantation, as well as to BMs as major homing sites of stem cells. Through dynamics analyses, I further demonstrated that the recruitment of the exogenous Lin^- cells to the inflamed skin occurs directly, with maintenance of the Lin^- phenotype, following transplantation, without passing through the BM, although some portion of these cells also migrate to the inflamed tissue via the BM. Another intriguing point about the dynamics of infused Lin^- cells is that the progenies undergo in situ expansion in the inflamed skin, as confirmed by the increase in number of the progenies and the presence of BrdU-incorporating cells at the inflamed sites even following treatment with the BM-egress blockers FTY720 and DOP. Therefore, while most previous

studies have focused on the recruitment and differentiation of HSCs at injured sites at fixed time points, the longitudinal study generates detailed information linking recruitment and subsequent in situ expansion and differentiation of exogenous HSCs. These systemic analyses of transplanted Lin^- cells in the dermatitis recipients revealed expansion of the progenies in situ in the inflamed skin and in the BM. Moreover, they undergo similar kinetics of myeloid differentiation at the two locations. These almost synchronous dynamics of transplanted Lin^- cells suggest that systemic soluble factors present in the recipients regulate such activities. Chemokines (e.g., CXCL12), growth factors (e.g., G/M-CSF), and pro-inflammatory cytokines (e.g., IFNα /β , TNF-α , and IL-1) produced at the site of inflammation induce mobilization of HSCs from the BM [52]. Pro-inflammatory cytokines such as IFN-α , IL-1 and IFN-γ could also induce HSCs and Lin^- cells to enter the cell cycle [52]. Moreover, these inflammatory cytokines promote biased differentiation of Lin^- cells into myeloid precursors and expansion of granulocytes [52]. Thus, I believe that the elevated levels of inflammatory cytokines, including TNF-α and IL-1, in the blood of DNCB-induced dermatitis mice (Fig.

1) regulate their recruitment to inflamed sites and subsequent expansion, as well as promote myeloid differentiation. Importantly, I revealed that the majority of progenies of transplanted Lin^- cells were of the $CD115^+CD11b^+Ly6G^{int}Ly6C^{hi}$ phenotype in the inflamed skin on days 5–7, when skin inflammation was most severe. Moreover, gene expression profiles and the suppressive function of these cells supported their identification as immune-suppressive MDSCs. In parallel flow cytometric analyses of $CD45.2^+$ cells of recipient origin, the recipient-derived $CD11b^+$ cells in inflamed skin had cellular compositions similar to those of the transplanted Lin^+ cells (Fig. 6) on days 5 and 7 post-transplantation *(data not shown).* Therefore, reduced CD3 transcript levels in the inflamed skin and expedited skin regeneration in mice transplanted with Lin− cells are concluded to be the outcomes of suppressive activity of the MDSCs newly generated from transplanted Lin^- cells, over T cell activation and inflammation. This suggested an immune-suppressive role of MDSCs in a skin inflammation model, consistent with previous reports of an anti-inflammatory function of $CD11b^+Ly6G^+Ly6C^+$ MDSCs in disease models, including

infection [56]. The fact that differentiation of exogenous Lin^- cells into $CD115^+CD11b^+Ly6G^{int}Ly6C^{hi}$ cells was greater in the inflamed skin than in BM suggests that local inflammation enhanced this differentiation. For example, TLR/MyD88 signaling was related to MDSC expansion, as shown by significant expansion of suppressive MDSCs after high-dose LPS treatment in an airway disease model. Consistently, when I transplanted Lin^- cells isolated from MyD88-deficient mice, the drastic cellular expansion in the inflamed skin usually observed after transplantation of wild-type Lin^- cells was impaired (unpublished data). Since homeostatic proteins, such as high mobility group box 1 and purinergic receptors, secreted into the extracellular milieu can induce TLR-mediated signaling [57], local proteins released from the damaged skin tissues are considered to trigger in situ MDSC differentiation and expansion of Lin^- cells in the inflamed area. In agreement with the view that MDSCs are at an immature differentiation stage [58], $CD11b^+Ly6G^{int}Ly6C^+CD115^+$ MDSCs represented a major proportion of Lin^- progeny on days 5 and 7, when these progenies showed extensive proliferation in situ and before the emergence of other cell lineages on day 14, highlighting the

extreme plasticity and proliferative potential of the MDSCs. On day 14 post-transplantation, Ly6G levels in the $CD11b^{+}Ly6G^{int}Ly6C^{+}$ cells were slightly increased, and $CD11b^{+}Ly6G^{hi}Ly6C^{int}$ neutrophils became the predominant population. As neutrophils have a very short life span, the decrease in luminescence signals at the site of inflammation following the peak at day 14 post-transplantation can be ascribed to differentiation of B6.LucTg Lin^{-} cells into short-lived cell types, such as neutrophils. However, faint signals remained evident on days 35 and 42 post-transplantation *(data not shown),* although luminescence signals were significantly diminished at both inflamed sites and in BM by day 28 post-transplantation (Fig. 2C). These results suggest that certain rare progenies of transplanted Lin^{-} cells may persist in the regenerated skin and BM as stem cells. Alternatively, the cells emitting the faint signals may be those that have trans-differentiated into parenchymal cells incorporated into the dermis, producing collagen III15 and/or other cellular components necessary for skin regeneration [59]. Further studies are necessary to characterize the cells emitting the reminiscent signals in the inflamed skin after the inflammation

subsided significantly and to provide direct evidence of trans-differentiation in the context of dermatitis mice. Nonetheless, this study clearly demonstrates that the therapeutic effects and enhanced skin regeneration facilitated by Lin^- cells stems from their in situ differentiation into anti-inflammatory MDSCs. Collectively, I demonstrate dynamic migration, expansion, and differentiation of transplanted Lin^-cells in recipients with skin inflammation, suggesting that skewed differentiation into immune-suppressive $CD11b^+Ly6G^{int}Ly6C^+$MDSCs with enhanced CD115 expression correlates the therapeutic effect of transplanted Lin^- cells. This study provides an overview of the in vivo dynamics and insights into the activity of transplanted HSCs, and suggests that HSC transfer can be a potential treatment modality for serious diseases such as psoriasis and in skin graft-versus host disease (GVHD).

REFERENCES

1. Kaech, S.M., Wherry, E.J., and Ahmed, R. (2002). Effector and memory T-cell differentiation: implications for vaccine development. Nat Rev Immunol *2*, 251-262.
2. Bevan, M.J. (2004). Helping the CD8(+) T-cell response. Nat Rev Immunol *4*, 595-602.
3. Kaech, S.M., and Cui, W. (2012). Transcriptional control of effector and memory CD8+ T cell differentiation. Nat Rev Immunol *12*, 749-761.
4. Schoenberger, S.P., Toes, R.E., van der Voort, E.I., Offringa, R., and Melief, C.J. (1998). T-cell help for cytotoxic T lymphocytes is mediated by CD40-CD40L interactions. Nature *393*, 480-483.
5. Bennett, S.R., Carbone, F.R., Karamalis, F., Flavell, R.A., Miller, J.F., and Heath, W.R. (1998). Help for cytotoxic-T-cell responses is mediated by CD40 signalling. Nature *393*, 478-480.
6. Feau, S., Garcia, Z., Arens, R., Yagita, H., Borst, J., and Schoenberger, S.P. (2012). The CD4(+) T-cell help signal is transmitted from APC to CD8(+) T-cells via CD27-CD70 interactions. Nat Commun *3*, 948.
7. Filatenkov, A.A., Jacovetty, E.L., Fischer, U.B., Curtsinger, J.M., Mescher, M.F., and Ingulli, E. (2005). CD4 T cell-dependent conditioning of dendritic cells to produce IL-12 results in CD8-mediated graft rejection and avoidance of tolerance. J Immunol *174*, 6909-6917.
8. VanderVegt, F.P., and Johnson, L.L. (1993). Induction of long-term H-Y-specific tolerance in female mice given male lymphoid cells while transiently depleted of CD4+ or CD8+ T cells. J Exp Med *177*, 1587-1592.
9. Janssen, E.M., Droin, N.M., Lemmens, E.E., Pinkoski, M.J., Bensinger, S.J., Ehst, B.D., Griffith, T.S., Green, D.R., and Schoenberger, S.P. (2005). CD4+ T-cell help controls CD8+ T-cell memory via TRAIL-mediated activation-induced cell death. Nature *434*, 88-93.
10. Fuse, S., Tsai, C.Y., Molloy, M.J., Allie, S.R., Zhang, W., Yagita, H., and Usherwood, E.J. (2009). Recall responses by helpless memory CD8+ T cells are restricted by the up-regulation of PD-1. J Immunol *182*, 4244-4254.
11. Sacks, J.A., and Bevan, M.J. (2008). TRAIL deficiency does not rescue impaired CD8+ T cell memory generated in the absence of CD4+ T cell help. J Immunol *180*, 4570-4576.
12. Choi, E.Y., Yoshimura, Y., Christianson, G.J., Sproule, T.J., Malarkannan, S., Shastri, N., Joyce, S., and Roopenian, D.C. (2001). Quantitative analysis of the immune response to mouse non-MHC transplantation antigens in vivo: the H60

histocompatibility antigen dominates over all others. J Immunol *166*, 4370-4379.
13. Kedl, R.M., Rees, W.A., Hildeman, D.A., Schaefer, B., Mitchell, T., Kappler, J., and Marrack, P. (2000). T cells compete for access to antigen-bearing antigen-presenting cells. J Exp Med *192*, 1105-1113.
14. Choi, E.Y., Christianson, G.J., Yoshimura, Y., Sproule, T.J., Jung, N., Joyce, S., and Roopenian, D.C. (2002). Immunodominance of H60 is caused by an abnormally high precursor T cell pool directed against its unique minor histocompatibility antigen peptide. Immunity *17*, 593-603.
15. Choi, E.Y., Christianson, G.J., Yoshimura, Y., Jung, N., Sproule, T.J., Malarkannan, S., Joyce, S., and Roopenian, D.C. (2002). Real-time T-cell profiling identifies H60 as a major minor histocompatibility antigen in murine graft-versus-host disease. Blood *100*, 4259-4265.
16. Ryu, S.J., Jung, K.M., Yoo, H.S., Kim, T.W., Kim, S., Chang, J., and Choi, E.Y. (2009). Cognate CD4 help is essential for the reactivation and expansion of CD8 memory T cells directed against the hematopoietic cell-specific dominant minor histocompatibility antigen, H60. Blood *113*, 4273-4280.
17. Choi, J.H., Ryu, S.J., Jung, K.M., Kim, S., Chang, J., Kim, T.W., and Choi, E.Y. (2009). TCR diversity of H60-specific CD8 T cells during the response evolution and influence of CD4 help. Transplantation *87*, 1609-1616.
18. Kouskoff, V., Signorelli, K., Benoist, C., and Mathis, D. (1995). Cassette vectors directing expression of T cell receptor genes in transgenic mice. J Immunol Methods *180*, 273-280.
19. Jeon, J.Y., Jung, K.M., Chang, J., and Choi, E.Y. (2011). Characterization of CTL Clones Specific for Single Antigen, H60 Minor Histocompatibility Antigen. Immune Netw *11*, 100-106.
20. Zloza, A., Kohlhapp, F.J., Lyons, G.E., Schenkel, J.M., Moore, T.V., Lacek, A.T., O'Sullivan, J.A., Varanasi, V., Williams, J.W., Jagoda, M.C., et al. (2012). NKG2D signaling on CD8(+) T cells represses T-bet and rescues CD4-unhelped CD8(+) T cell memory recall but not effector responses. Nat Med *18*, 422-428.
21. Anderson, C.C., and Matzinger, P. (2001). Immunity or tolerance: opposite outcomes of microchimerism from skin grafts. Nat Med *7*, 80-87.
22. Yoo, K.I., Jeon, J.Y., Ryu, S.J., Nam, G., Youn, H., and Choi, E.Y. (2015). Subdominant H60 antigen-specific CD8 T-cell response precedes dominant H4 antigen-specific response during the initial phase of allogenic skin graft rejection. Exp Mol Med *47*, e140.
23. Kim, J., Ryu, S.J., Oh, K., Ju, J.M., Jeon, J.Y., Nam, G., Lee, D.S., Kim, H.R., Young Kim, J., Chang, J., et al. (2015). Memory

programming in CD8(+) T-cell differentiation is intrinsic and is not determined by CD4 help. Nat Commun *6*, 7994.
24. Roopenian, D., Choi, E.Y., and Brown, A. (2002). The immunogenomics of minor histocompatibility antigens. Immunological reviews *190*, 86-94.
25. Bleakley, M., and Riddell, S.R. (2004). Molecules and mechanisms of the graft-versus-leukaemia effect. Nature reviews. Cancer *4*, 371-380.
26. Speir, J.A., Stevens, J., Joly, E., Butcher, G.W., and Wilson, I.A. (2001). Two different, highly exposed, bulged structures for an unusually long peptide bound to rat MHC class I RT1-Aa. Immunity *14*, 81-92.
27. Apostolopoulos, V., Yuriev, E., Ramsland, P.A., Halton, J., Osinski, C., Li, W., Plebanski, M., Paulsen, H., and McKenzie, I.F. (2003). A glycopeptide in complex with MHC class I uses the GalNAc residue as an anchor. Proceedings of the National Academy of Sciences of the United States of America *100*, 15029-15034.
28. Boesteanu, A., Brehm, M., Mylin, L.M., Christianson, G.J., Tevethia, S.S., Roopenian, D.C., and Joyce, S. (1998). A molecular basis for how a single TCR interfaces multiple ligands. Journal of immunology *161*, 4719-4727.
29. Evavold, B.D., Sloan-Lancaster, J., and Allen, P.M. (1993). Tickling the TCR: selective T-cell functions stimulated by altered peptide ligands. Immunology today *14*, 602-609.
30. Garcia, K.C., Teyton, L., and Wilson, I.A. (1999). Structural basis of T cell recognition. Annual review of immunology *17*, 369-397.
31. Sawicki, M.W., Dimasi, N., Natarajan, K., Wang, J., Margulies, D.H., and Mariuzza, R.A. (2001). Structural basis of MHC class I recognition by natural killer cell receptors. Immunological reviews *181*, 52-65.
32. Klein, L., Kyewski, B., Allen, P.M., and Hogquist, K.A. (2014). Positive and negative selection of the T cell repertoire: what thymocytes see (and don't see). Nature reviews. Immunology *14*, 377-391.
33. Sebzda, E., Wallace, V.A., Mayer, J., Yeung, R.S., Mak, T.W., and Ohashi, P.S. (1994). Positive and negative thymocyte selection induced by different concentrations of a single peptide. Science *263*, 1615-1618.
34. Russell, P.S., Chase, C.M., Madsen, J.C., Hirohashi, T., Cornell, L.D., Sproule, T.J., Colvin, R.B., and Roopenian, D.C. (2011). Coronary artery disease from isolated non-H2-determined incompatibilities in transplanted mouse hearts. Transplantation *91*, 847-852.
35. Nelson, R.W., Beisang, D., Tubo, N.J., Dileepan, T., Wiesner,

D.L., Nielsen, K., Wuthrich, M., Klein, B.S., Kotov, D.I., Spanier, J.A., et al. (2015). T cell receptor cross-reactivity between similar foreign and self peptides influences naive cell population size and autoimmunity. Immunity *42*, 95-107.

36. Moon, J.J., Chu, H.H., Pepper, M., McSorley, S.J., Jameson, S.C., Kedl, R.M., and Jenkins, M.K. (2007). Naive CD4(+) T cell frequency varies for different epitopes and predicts repertoire diversity and response magnitude. Immunity *27*, 203-213.
37. Zehn, D., and Bevan, M.J. (2006). T cells with low avidity for a tissue-restricted antigen routinely evade central and peripheral tolerance and cause autoimmunity. Immunity *25*, 261-270.
38. Malherbe, L., Filippi, C., Julia, V., Foucras, G., Moro, M., Appel, H., Wucherpfennig, K., Guery, J.C., and Glaichenhaus, N. (2000). Selective activation and expansion of high-affinity CD4+ T cells in resistant mice upon infection with Leishmania major. Immunity *13*, 771-782.
39. Jensen, K.D., Sercarz, E.E., and Gabaglia, C.R. (2009). Altered peptide ligands can modify the Th2 T cell response to the immunodominant 161-175 peptide of LACK (Leishmania homolog for the receptor of activated C kinase). Mol Immunol *46*, 366-374.
40. Wauben, M.H., Joosten, I., Schlief, A., van der Zee, R., Boog, C.J., and van Eden, W. (1994). Inhibition of experimental autoimmune encephalomyelitis by MHC class II binding competitor peptides depends on the relative MHC binding affinity of the disease-inducing peptide. J Immunol *152*, 4211-4220.
41. de Haan, E.C., Moret, E.E., Wagenaar-Hilbers, J.P., Liskamp, R.M., and Wauben, M.H. (2005). Possibilities and limitations in the rational design of modified peptides for T cell mediated immunotherapy. Mol Immunol *42*, 365-373.
42. Ashton-Rickardt, P.G., Van Kaer, L., Schumacher, T.N., Ploegh, H.L., and Tonegawa, S. (1993). Peptide contributes to the specificity of positive selection of CD8+ T cells in the thymus. Cell *73*, 1041-1049.
43. Daniels, M.A., Teixeiro, E., Gill, J., Hausmann, B., Roubaty, D., Holmberg, K., Werlen, G., Hollander, G.A., Gascoigne, N.R., and Palmer, E. (2006). Thymic selection threshold defined by compartmentalization of Ras/MAPK signalling. Nature *444*, 724-729.
44. Wu, Y., Wang, J., Scott, P.G., and Tredget, E.E. (2007). Bone marrow-derived stem cells in wound healing: a review. Wound Repair Regen *15 Suppl 1*, S18-26.
45. Kavanagh, D.P., and Kalia, N. (2011). Hematopoietic stem cell homing to injured tissues. Stem Cell Rev *7*, 672-682.
46. Si, Y., Tsou, C.L., Croft, K., and Charo, I.F. (2010). CCR2

mediates hematopoietic stem and progenitor cell trafficking to sites of inflammation in mice. J Clin Invest *120*, 1192-1203.
47. Borlongan, C.V. (2011). Bone marrow stem cell mobilization in stroke: a 'bonehead' may be good after all! Leukemia *25*, 1674-1686.
48. Bucala, R., Spiegel, L.A., Chesney, J., Hogan, M., and Cerami, A. (1994). Circulating fibrocytes define a new leukocyte subpopulation that mediates tissue repair. Mol Med *1*, 71-81.
49. Contag, C.H., Spilman, S.D., Contag, P.R., Oshiro, M., Eames, B., Dennery, P., Stevenson, D.K., and Benaron, D.A. (1997). Visualizing gene expression in living mammals using a bioluminescent reporter. Photochem Photobiol *66*, 523-531.
50. Song, M.G., Kang, B., Jeon, J.Y., Chang, J., Lee, S., Min, C.K., Youn, H., and Choi, E.Y. (2012). In vivo imaging of differences in early donor cell proliferation in graft-versus-host disease hosts with different pre-conditioning doses. Mol Cells *33*, 79-86.
51. Chong, S.Z., Tan, K.W., Wong, F.H., Chua, Y.L., Tang, Y., Ng, L.G., Angeli, V., and Kemeny, D.M. (2014). CD8 T cells regulate allergic contact dermatitis by modulating CCR2-dependent TNF/iNOS-expressing Ly6C+ CD11b+ monocytic cells. J Invest Dermatol *134*, 666-676.
52. Baldridge, M.T., King, K.Y., and Goodell, M.A. (2011). Inflammatory signals regulate hematopoietic stem cells. Trends Immunol *32*, 57-65.
53. Gabrilovich, D.I., and Nagaraj, S. (2009). Myeloid-derived suppressor cells as regulators of the immune system. Nat Rev Immunol *9*, 162-174.
54. Ratajczak, M.Z., Lee, H., Wysoczynski, M., Wan, W., Marlicz, W., Laughlin, M.J., Kucia, M., Janowska-Wieczorek, A., and Ratajczak, J. (2010). Novel insight into stem cell mobilization-plasma sphingosine-1-phosphate is a major chemoattractant that directs the egress of hematopoietic stem progenitor cells from the bone marrow and its level in peripheral blood increases during mobilization due to activation of complement cascade/membrane attack complex. Leukemia *24*, 976-985.
55. Youn, J.I., Nagaraj, S., Collazo, M., and Gabrilovich, D.I. (2008). Subsets of myeloid-derived suppressor cells in tumor-bearing mice. J Immunol *181*, 5791-5802.
56. Serafini, P., Borrello, I., and Bronte, V. (2006). Myeloid suppressor cells in cancer: recruitment, phenotype, properties, and mechanisms of immune suppression. Semin Cancer Biol *16*, 53-65.
57. Wang, H., Bloom, O., Zhang, M., Vishnubhakat, J.M., Ombrellino, M., Che, J., Frazier, A., Yang, H., Ivanova, S., Borovikova, L., et al. (1999). HMG-1 as a late mediator of endotoxin lethality in

mice. Science *285*, 248-251.
58. Nefedova, Y., Nagaraj, S., Rosenbauer, A., Muro-Cacho, C., Sebti, S.M., and Gabrilovich, D.I. (2005). Regulation of dendritic cell differentiation and antitumor immune response in cancer by pharmacologic-selective inhibition of the janus-activated kinase 2/signal transducers and activators of transcription 3 pathway. Cancer Res *65*, 9525-9535.
59. Tamai, K., Yamazaki, T., Chino, T., Ishii, M., Otsuru, S., Kikuchi, Y., Iinuma, S., Saga, K., Nimura, K., Shimbo, T., et al. (2011). PDGFRalpha-positive cells in bone marrow are mobilized by high mobility group box 1 (HMGB1) to regenerate injured epithelia. Proc Natl Acad Sci U S A *108*, 6609-6614.

국문 초록

우리 몸은 면역의 항상성유지를 위하여 면역과 관용의 균형이 필요하다. 특히, 조직이식에서 동종이계의 항원에 대한 면역반응과 자가면역질환에서 자기세포에 대한 면역반응을 조절하기위한 면역관용을 이해하는 것은 중요한 의미를 갖는다. 기존의 많은 연구들에서 밝혀왔듯이, CD8 T 세포가 자극될 때, CD4 T 세포 도움은 CD8 T 세포의 질 높은 증식과 기능을 위해 중요하다. 우리는 우성 부조직적합항원, H60 이 세포항원으로서, CD8 T 세포의 반응을 위해 CD4 T 세포의 도움이 절대적으로 중요하다는 것을 선행 연구를 통해 밝혀왔다. 이 연구에서 나는 1 차 면역반응에서 CD4 help 가 결핍되었던 CD8 T 세포가 2 차 면역반응의 결함을 확인하였다. 또한 H60 특이적인 CD8 T 세포 반응의 억제가 다른 부조직적합항원에 대한 CD8 T 세포 반응은 모두 억제시킬 수 있음을 확인하였다. 이러한 면역관용현상은 이식편대숙주병과 피부조직이식에서 부조직적합항원에대한 이식거부반응이 억제되는 결과를 확인하였다.

H60 특이적 CD8 T 세포의 흉선에서의 발달과정에 대한 이해를 위해 H60 항원결정부위의 염기가 단일 치환된 펩타이드에 대한 H60 특이적 CD8 T 세포의 결합 활성도를 측정하였다. 그 중에서 4 번째 asparagine 이 histidine 으로 치환된 H60H 가 H60 특이적

CD8 T 세포와 낮은 결합 활성도를 갖는 부분적 작용물질 (Partial agonist)였다. H60H는 H60처럼 CD4 T 세포 도움의 의존성을 가지며 특이적 CD8 T 세포반응을 유도할 수 있었고, H60 특이적 CD8 T 세포와 약간의 TCR을 공유하고 있었다.

피부질환모델에서 T 세포 반응조절을 연구하기 하여 계열음성세포를 이식하였다. 이식한 계열음성세포는 감염부위에서 골수성세포로 분화하였고 CD8 T 세포 반응을 억제시키는 역할을 함으로써 피부질환이 완화되는 결과를 얻었다. 이 연구 결과들은 CD8 T 세포 반응의 발달과정에 대한 새로운 정보를 주고, 이를 통해 CD8 T 세포 조절을 이용한 치료에의 적용에 중요한 단서를 제공할 것으로 기대한다.

주요어 : 부조직적합항원, CD4 도움, 면역관용, 메모리 CD8 T cell 반응, 미분화 골수성 세포

학 번 : 2009-21884